THE IMPACT OF TRANSMISSION PROTECTION SYSTEM RELIABILITY ON POWER SYSTEM RESILIENCE

A Dissertation

by

MOHAMMAD TASDIGHI

Submitted to the Office of Graduate and Professional Studies of
Texas A&M University
in partial fulfillment of the requirements for the degree of

DOCTOR OF PHILOSOPHY

Chair of Committee,	Katherine Davis
Committee Members,	Thomas Overbye
	Kamran Entesari
	Ana Goulart
Head of Department,	Miroslav Begovic

August 2018

Major Subject: Electrical Engineering

ABSTRACT

Power transmission operation regimes are being changed for various technical and economic reasons seeking an improved power system resilience as a goal. However, some of these changes introduce new challenges in maintaining conventional transmission protection system dependability and security when meeting the operating complexities affecting power system resilience. Frequently evolving network topology, as a result of multiple switching actions for corrective, predictive and post event purposes, as well as high penetration of distributed generation into the system are considered as major contradictory changes from the legacy transmission protection standpoint.

This research investigates the above-mentioned challenges and proposes effective solutions to improve the transmission protection reliability facing the above-mentioned risks and power system resilience consequently. A fundamental protection scheme based on the Hierarchically Coordinated Protection (HCP) concept is proposed to illustrate various approaches to predictive, adaptive and corrective protection actions aimed at improving power system resilience. Novel computation techniques as well as intelligent machine-learning algorithms are employed in proposing predictive, adaptive, and corrective solutions which fit various layers of the HCP concept and incorporate a fundamental HCP-based approach to supervise the legacy transmission protection function for a dynamic balance between dependability and security. The proposed predictive, adaptive, and corrective protection approaches are tested and verified on various systems, including real-life and IEEE test systems, and their performance effectiveness is compared with the state of the art.

DEDICATION

To my mother and father, Shokooh and Mohammadreza, and my beloved wife, Atrin, for their ever-encouraging support

ACKNOWLEDGMENTS

I would like to acknowledge my committee chair, Dr. Davis, and my committee members, Dr. Overbye, Dr. Entesari, and Dr. Goulart, as well as Dr. Kezunoivc, Dr. Bhattacharyya, Dr. Huang, and Dr. Butenko for their guidance and support throughout the course of this research.

Appreciation also goes to my friends and colleagues and the department faculty and staff for making my time at Texas A&M University a great experience. I would especially thank Dr. Gurunath Gurrala and Dr. Ashok Gopalakrishnan for their help along the way.

I would like to thank all my friends who made my time in College Station enjoyable and fun. Thank you Ashkan, Payman, Omid, Farzad, Mani, Paria, and Sajad. Without you, life in college would have been much harder.

Thanks also go to my beloved parents and wife. I wouldn't have achieved what I have done without their encouragement.

CONTRIBUTORS AND FUNDING SOURCES

Contributors

This work was supported by a dissertation committee consisting of Professor Davis (advisor), Professor Overbye, and Professor Entesari of Department of Electrical and Computer Engineering and Professor Goulart of Department of Engineering Technology and Industrial Distribution. Furthermore, this work was benefited from instructions given by Professor Kezunovic, Professor Huang, Professor Bhattacharyya, and Professor Butenko.

All other work conducted for the dissertation was completed by the student independently.

Funding Sources

This work was supported in part by the from the Advanced Research Projects Agency-Energy (ARPA-E), U.S. Department of Energy (DOE), under the Green Electricity Network Integration (GENI) project “Robust Adaptive Topology Control”, ARPA-E award no. DE-AR0000220.

NOMENCLATURE

Nomenclature 1: General

DG	Distributed Generation
PV	Photo Voltaic
TSO	Transmission System Operator
SVM	Support Vector Machine
HCP	Hierarchically Coordinate Protection
DoI	Distance of Impact
PCC	Point of Common Coupling
DIREC	Disturbance Impact and Resiliency Evaluation Curve

Nomenclature 2: Section 5

Nbu	Number of buses in the network
Nbr	Number of branches in the network
V_{LL}	Rated line-to-line voltage
I_{rating}	The line current rating
Z^{30}_{relay}	Relay reach in primary ohms at a power factor angle of 30 degrees
Z_1	Zone 1 phase reach in primary ohms
Z_2	Zone 2 phase reach in primary ohms
Z_3	Zone 3 phase reach in primary ohms
Z^l_2	Zone 2 phase reach based on line ohms only
Z^{app}_2	Zone 2 phase reach based on the remote bus fault apparent impedance
Z^l_3	Zone 3 phase reach based on line ohms only
$Z^{app_{bus}}_3$	Zone 3 phase reach based on apparent impedance of next adjacent bus faults
$Z^{app_{end}}_3$	Zone 3 phase reach based on apparent impedance of next adjacent Line-end faults
z_l	Impedance of the line
z^{adj}_{li}	Impedance magnitude of the next adjacent line *i*
z^{adj}_{pi}	Line ohms path magnitude to the next adjacent bus *i*
z_{rem}	Apparent impedance for three phase fault on remote bus
z^{adj}_i	Apparent impedance for three phase fault on next adjacent bus *i*
$z^{adj}_{end_i}$	Apparent impedance for three phase line-end fault on the next adjacent line *i*

N^{adj}	Number of next adjacent buses
Z^{col}	Required updated column of Z_{bus} corresponding to a line-end fault implementation
$V^{post}{}_n$	Post-fault voltage of bus n
$V^{pre}{}_n$	Pre-fault voltage of bus n
$R_{i\text{-}j}$	Distance relay looking from bus i to bus j
Y_{ij}	Admittance of the line between buses i and j
Y_{sh}	Shunt capacitance in *pi* model of the line

TABLE OF CONTENTS

Page

LIST OF FIGURES

Page

LIST OF TABLES

Page

1. INTRODUCTION

1.1. Problem Statement

Due to increase in power system complexity, it is becoming more obvious that the classical reliability-based perspective alone would not suffice ensuring a continuous power supply [1-2]. The emerging economic and environmental concerns have resulted in introduction of renewables, distributed generation, microgrids and other electricity grid infrastructure changes creating operating uncertainties and complexities. As a consequence, it is required from the power system to be resilient against the high-impact low-probability events, as well as conventional threats, and hence to surpass the existing performance [1-2]. Various aspects of power system such as protection, operation, planning, etc. should function properly to improve system resilience. The focus of this dissertation is on the role of transmission protection reliability in this pursue.

Investigating major failures, such as cascading events, in the recent history of the power system operation has revealed that the protection malfunction has been a contributing factor in the majority of the failures [3-5]. Maintaining the balance between protection dependability and security has always been a challenge specially under the new operating complexities [5-6]. The conventional conservative viewpoint of outweighing protection dependability over security does not fit the new concept of resiliency and a fundamental approach is required to strike a balance between dependability and security for improving protection reliability and system resilience consequently.

1.2. Research Objectives

The focus of this dissertation is to identify the main challenges against proper

function of legacy transmission protection system under increased system complexities as a result of alleviating operating difficulties towards improving power system resilience. The idea is to propose a fundamental protection approach which supervises the legacy transmission protection function to dynamically balance the protection dependability and security. A combination of protection schemes including predictive protection, adaptive protection, and corrective protection will be proposed to incorporate a HCP based approach which prevents relay misoperation under high-impact low-probability events and supports power system resilience consequently.

1.3. Dissertation Outline

The rest of this dissertation is organized as follows. Section 2 reviews the power system resilience and protection reliability concepts as well as the correlation between them. The features of a resilient control system, power system protection in this study, are discussed and the impact of improving protection reliability on each of the features is explained. Furthermore, the system complexities which are considered as main contradictory changes from the legacy transmission protection standpoint are introduced and their impact on the proper function of the legacy transmission protection is discussed. Section 3 formulates the problem to be solved in addressing the system complexities under consideration. The concept of HCP and the theoretical framework of the proposed fundamental approach utilizing HCP concept to supervise legacy transmission protection function is explained. Section 4 surveys the state of the art and previous research efforts which can be considered as potential solutions for various layers of the fundamental HCP-based approach and the areas which have to be explored more are identified. Sections

5, 6, and 7 propose novel protection schemes as solutions which fit the predictive, adaptive, and corrective layers of the fundamental HCP-based supervisory approach respectively. At each of these Sections, the performance effectiveness of the proposed solution compared to the state of the art is discussed. The concluding remarks and main contributions of the dissertation are summarized in Section 8. Future research trends are also discussed in this Section. References are brought at the end.

2. BACKGROUND

2.1. Power System Resilience

There is not a universally accepted definition for the concept of resilience as it has been defined in several ways. According to the UK Energy Research Center [7], resilience is defined as "the capacity of an energy system to tolerate disturbance and to continue to deliver affordable energy services to consumers. A resilient energy system can speedily recover from shocks and can provide alternative means of satisfying energy service needs in the event of changed external circumstances." Reference [8] defines a resilient system as a system which degrades gradually, and not abruptly, when it experiences stressed conditions and it is able to restore back into its normal state thereafter. The National Infrastructure Advisory Council (NIAC), USA [9], adds another property to the resilient system definition where a resilient system learns from its previous lessons and experiences under major disturbances and uses this knowledge to adapt and fortify itself to prevent or mitigate the consequences of a similar event in the future. The Cabinet Office U.K. defines a resilient system as a system able to ". . .anticipate, absorb, adapt to and/or rapidly recover from a disruptive event" [10]. Resilience is defined in [11] as the "robustness and recovery characteristics of utility infrastructure and operations, which avoid or minimize interruptions of service during an extraordinary and hazardous event". The US National Academies report considers a resilient system the one which plans and prepares for a disruptive event, absorbs it and is able to recover from it. More importantly, it adapts itself for similar future events [12].

Referring to several definitions developed for resilience in the power system area,

it could be realized that unlike reliability which is a static concept, resilience has a dynamic, unfolding, and time-variant nature. Reliability can be defined as the ability of the power system to deliver electricity in the quantity and with the quality demanded by users [2]. It is generally measured by interruption indices defined by IEEE standards [13]. Reliability focuses on keeping the lights on in a consistent manner. This is a binary view of the system performance where systems are either functional or failed. On the other hand, resiliency suggests the idea that there is a flexible continuum between functional and failed, so moves beyond the rigid duality promoted by reliability. The main features of resilience are robustness (withstand low probability but high consequence events), resourcefulness (effectively manage a disturbance as it unfolds), rapid recovery (get things back to normal as fast as possible after the disturbance), and adaptability (absorb new lessons from a catastrophe).

2.2. Protection System Reliability

Our view of protection system reliability focuses on dependability and security [6,14]. A protection system operating correctly in the case of faults within its protection zone is defined as being dependable [15]. The security, on the other hand, focuses on preventing the protection system's incorrect operation for faults out of protected zone or for normal (no-fault) operating conditions [16].

Protection systems must be fundamentally designed to be both dependable and secure [17]. Overall design must strike a balance between dependability and security because it has been shown that relay designs can only meet one criteria at the expense of the other. Dependability based protection system failures can result in longer fault clearing

times and isolation of additional elements of the electric system. Security-based protection system failures can result in isolation of healthy elements of the electric system.

Figure 1 shows an example of dependability-type failure of a protection system. The fault on line one is supposed to be detected by relays at both ends of the line and cleared by opening the corresponding breakers. However, if relay at substation 2, R2, fails to operate for any reason, then the backup protective devices, relays on generator, substation 3 and 4, R4 and R6, will clear the fault with a delay and also cause extended extent of outage by putting the generator, and lines 2 and 3 out of service.

Figure 2 shows an example of a security-based failure of a protection system. In this example, the fault on line 1 is being cleared by relays at both ends as it is supposed to. However, as a result of a security-failure, the relay at substation 4, R4, is also acting on the fault which is not in its primary protection zone. The operation of relay at substation 3

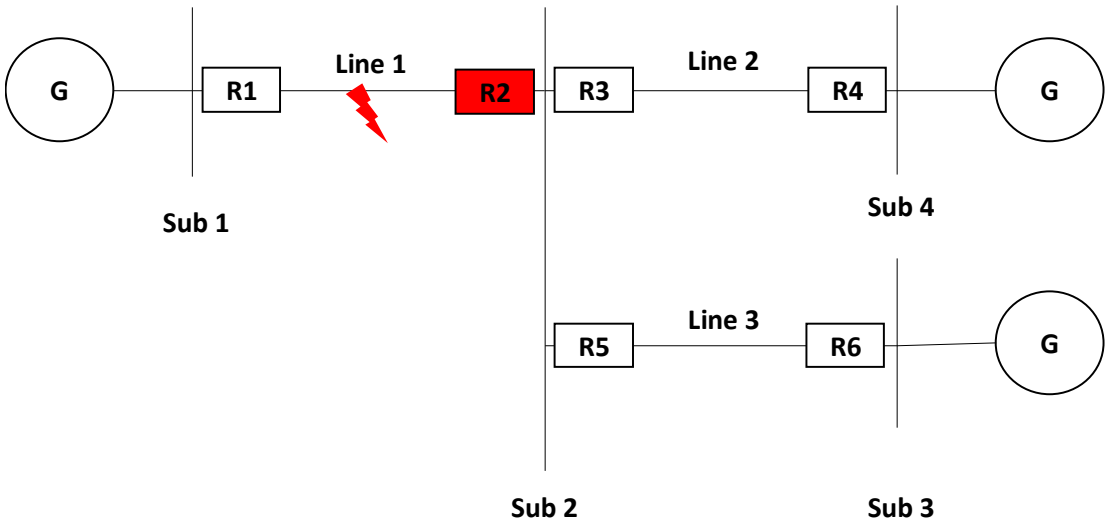

Figure 1. Dependability-type failure

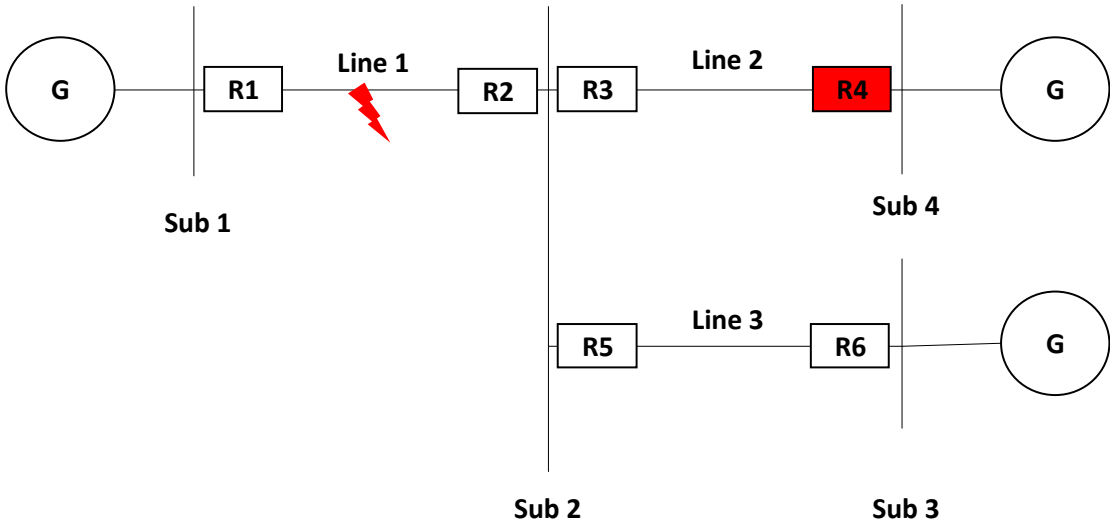

Figure 2. Security-type failure

will cause unnecessary outage of the healthy line 2 and extended extent of outage as well.

2.3. Protection System Reliability's Role in Power System Resilience

An extensive study of the major disturbances and blackouts in the recent history shows that frequently they have been associated with both dependability and security-based protection system failures [3-5]. Relay misoperation is known to be a contributing factor in 75 percent of the major disturbances in North America [3-5]. During abnormal conditions, the backup relays sometimes cannot differentiate faults from no-fault conditions (balance between dependability and security is inadequate), such as when overload and large power swings occur. It has been noted that while redundancy (providing backup protection and improving dependability) reduces the probability of a dependability-based protection system failure, it may increase the probability of a security-based protection system failure [5-6]. As a result, finding the balance between dependability and security of protective relay operation remains a challenge.

Following a disturbance, the system may experience a transition between various operating states based on the severity of the disturbance [2]. The state of the system depends on how it was designed and how it is operated. These choices influence whether and how service is degraded during a disruption, how quickly it recovers, and how completely it recovers. For example, an electricity grid system that is designed with more redundancy, operated with more contingencies for backup, and designed with recovery in mind might experience a lesser and briefer disruption and, if so, would be more resilient than a system that has less redundancy, has fewer backups, and is more difficult to rebuild. Figure 3 shows the change of the resilience on a resilience curve as the system transitions between the various states unfold. When the system is operating at normal state, i.e. operational constraints as well as security margins are satisfied and respected, the resiliency level is high. The system is robust enough to handle a single (N-1) disturbance

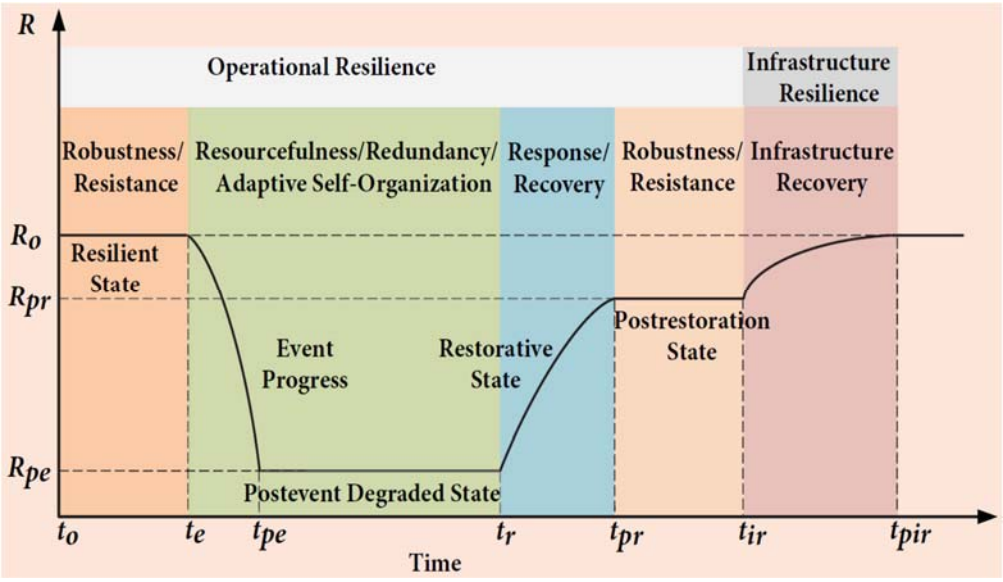

Figure 3. System's resilience curve following a disturbance

effectively. Following the disturbance, resiliency degrades depending on the severity of the disturbance and the system enters the post-event state. Resourcefulness, redundancy, and adaptive self-organizing can play a critical role at this state to provide opportunities for implementing corrective, preventive, emergency, or in extreme mitigating actions to minimize the degradation level ($R_o - R_{pe}$) before restoration process begins. Finally, after the disturbance resulted in a partial or complete outage the restorative actions should be taken to restore the system into normal conditions and recover its highest resiliency.

To better clarify the impact of protection reliability on system's resilience, we can compare the legacy protection reliability-based perspective with what the requirements for resilience asks for today. While the legacy protection on transmission may be able to handle the N-1 contingency case without causing any misoperation, it may not be able to cope with N-m contingency cases (high-impact low-probability events) effectively. In other words, statically predetermined balance between dependability and security might not meet the system's resilience criteria necessarily. This is simply because such balance does not exist statistically between the numerous N-m contingency cases in a real-life power system. In other words, it has to adapt and fine tune itself as the system's conditions evolve. As Figure 3 shows, the system's resilience is characterized by resiliency level at various states of the system as well as the transition time between the states. Maintaining the balance between protection dependability and security minimizes resilience degradation level ($R_o - R_{pe}$) and improves the gradual degradation by increasing degradation time ($t_{pe} - t_e$) as the system experiences N-m contingencies. It does so by preventing any additional stress on the system as a consequence of protection misoperation

as the disturbances are unfolding.

2.4. Protection System Reliability under System's Operating Complexities

Increased system complexities introduced to alleviate the operating difficulties, and improve system resilience ultimately, could become a counterproductive for proper functioning of conventional protection schemes and maintaining protection reliability which in turn may hurt the system resilience. To smooth the way of implementing these complexities in power systems operation, the challenges of maintaining proper operation of conventional protection schemes should be investigated and resolved. The complexities under consideration in this research are: 1) more frequent network topology changes as a result of switching actions, 2) high penetration of DGs (renewables specifically) into power systems, and 3) required sensitive anti-islanding controls and measures on DG interconnections according to the standards.

2.4.1. Evolving Network Topology

Multiple switching actions for various objectives such as avoiding congestion and mitigating cascades [18-19], preventing load-shedding [20-21], reducing the operation cost [22], supporting maintenance purposes [23-24], etc. is a big operational change which is gaining much attention these days. However, it also could be considered as one of the major causes of deterioration of reliability of the legacy transmission protection operation [25]. Evolving network topology may cause a change in the network short circuit value and affect setting coordination of the distance relays consequently [26-27]. The network relay settings that are set for a base network topology, might not be adequate for an evolving topology and the protection reliability might get affected. Revisiting the setting

coordination adequacy for evolving network topology seems to be critical in assuring that such an operating complexity does not affect resiliency. It should be noted that the power system fundamental (base) topology has been grown over decades based on the critical goal of having a stable system to provide the electricity for the end users as much as possible. Hence, the concept of achieving an optimal base topology which already takes into account the protection concerns and other challenges can be considered as a future trend of the power system which is out of scope of this study.

A case study on the New-England 39-bus system, shown in Figure 4, is discussed here for a better understanding of the problem under consideration. The testing scenario is to assess the setting coordination adequacy for the relays $R_{27\text{-}26}$ and $R_{26\text{-}28}$ for a fault at x = 0.8 of the line 28-29 under the base network topology, i.e. all lines in service, and a

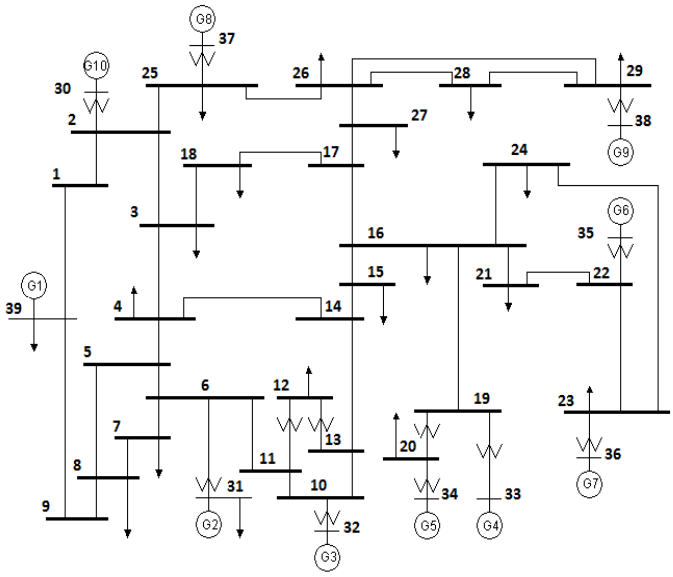

Figure 4. One-line diagram of New-England 39 bus system

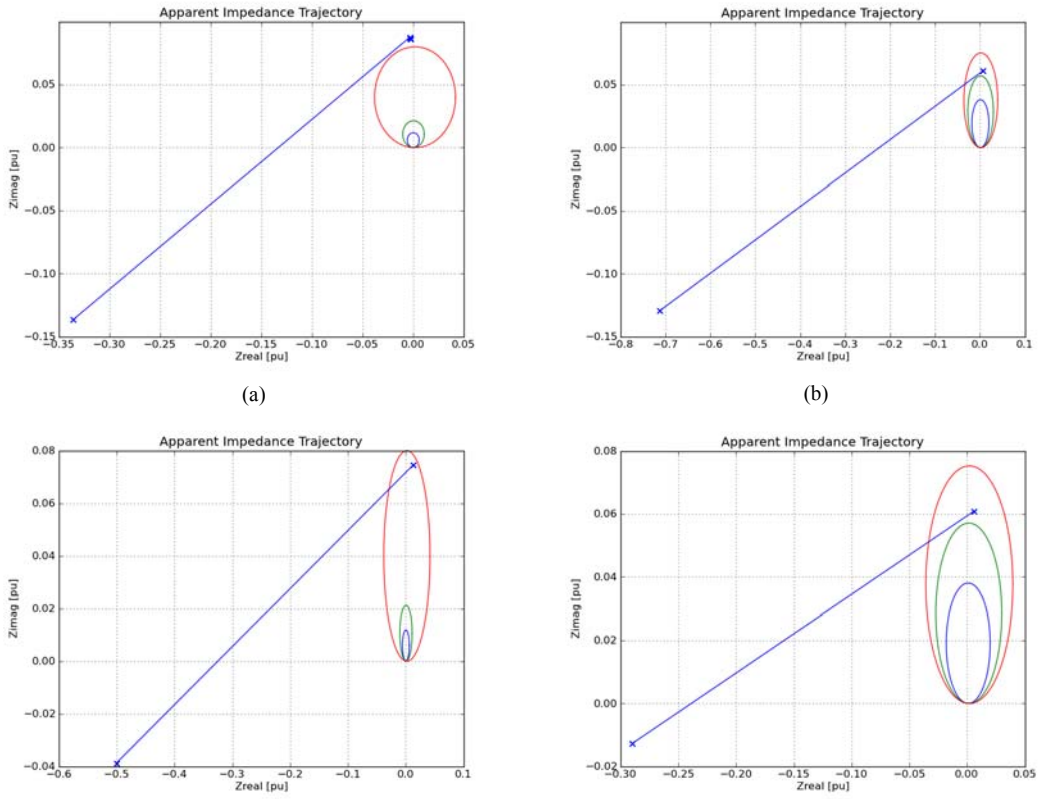

Figure 5. Apparent impedance trajectory seen by $R_{27\text{-}26}$ and $R_{26\text{-}28}$; (a)-(b) for base network topology; (c)-(d) for two lines 17-18 and 26-29 switched out

change in the network topology by switching out the lines 17-18 and 26-29. Figure 5 (a) and (b) show the apparent impedance trajectory during the fault scenario under the base network topology for the relays $R_{27\text{-}26}$ and $R_{26\text{-}28}$ respectively. As it could be seen the setting coordination has been maintained with regards to the back-up protection for the primary relay $R_{28\text{-}29}$. However, following the topology change, both primary and backup relays are seeing the same fault in their third zone as it could be seen from Figure 5 (c) and (d) which is a miss-coordination and a thread to the protection reliability in case of the primary

relay/breaker failure. This highlights the importance and critical role of revisiting the setting coordination adequacy for an evolving network topology to predict and plan for the protection vulnerabilities under future unpredictable faults and fulfilling a resilient operation of the power system consequently.

2.4.2. High Penetration of Renewables

It has been recognized that employing renewables as new sources of power will be significantly beneficial from both economic and environmental perspectives [28-30]. The new trend is towards incorporating significant amounts of renewables into power systems [28-30]. However, it is still a challenge to realize how to deal with their uncertain generation and its consequences on the power system resilient operation. As an example, from the transmission protection point of view, the uncertain power generation by renewables is translated into varying power flows on the lines that in case of significant changes could become a threat to proper operation of distance relay backup zones with respect to their loading limits. Currently, the distance relays are set in a network assuming that the loading of the lines are known [31]. The transmission protection schemes should be able to predict the protection vulnerabilities as a result of major power flow changes to maintain the protection dependability and security.

2.4.3. Anti-Islanding Protection Schemes

Microgrid technology and decentralized energy systems with the large-scale deployment of distributed energy resources and decentralized control can play a key role in providing resilience against system disturbances [2]. However, the enforcement of the standards for DG interconnection protection and control measures for detaching DGs from

the grid under certain circumstances might act as a threat to upstream protection coordination as DG penetration increases in the system [28-30]. As an example, a severe voltage sag propagating to the distribution side from the transmission level as a result of a three-phase fault can interfere with sensitive under-voltage based anti-islanding protection schemes and cause simultaneous tripping on DG units. NERC has recently reported an unintended tripping of 1200 MW PV generation from the grid as a consequence of sensitive under frequency/voltage protection measures (anti-islanding protection schemes) on the interconnection point [32]. The sudden increase of power flow to compensate the lack of DG in the system which is already under stress of previous disturbance as well as probable loss of synchronism between generators could initiate distance relay misoperation and lead to cascade events. This is among immediate concerns of some ISOs which have high penetration of DGs, PVs specifically, in their markets [33].

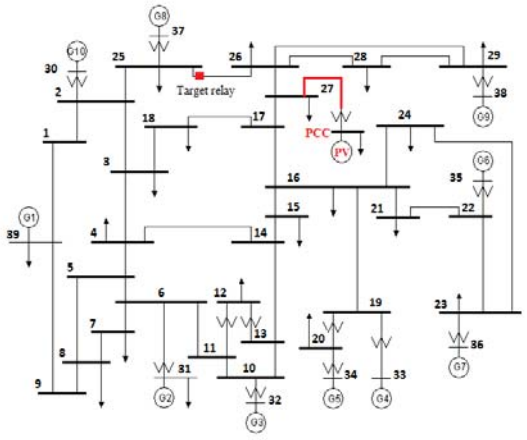

Figure 6. New-England system with high penetration of DGs

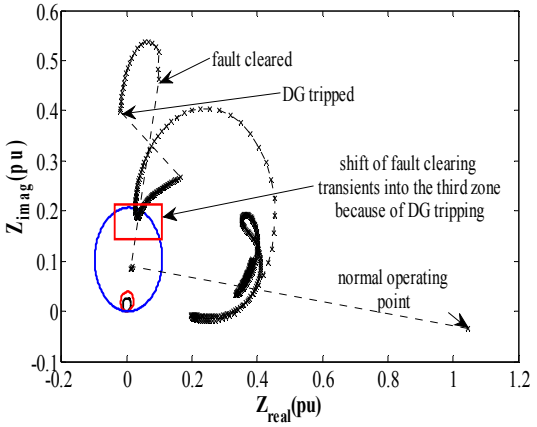

Figure 7. The apparent impedance trajectory for a DG tripping scenario following a short circuit in the system

A case study on the New-England 39-bus system is demonstrated here for a better understanding of the problem under consideration. Significant aggregated PV generation is assumed be located on the bus 27 of the system, as shown in Figure 6. Figure 7 shows the apparent impedance trajectory seen by a target relay in the vicinity of the DG PCC (Relay 25-26) when a 3-phase fault happens in the middle of the line 26-29, which clears after 0.2 second by tripping the line 26-29 out, and then 0.27 second later 150 MW PV is tripped. As Figure 7 shows, the impedance trajectory after the fault clearing has been shifted into the third zone of the relay, which can initiate a false trip as a result. According to measurements from the simulation, the target relay sees the impedance trajectory in its third zone for about 60 cycles which is critically close to issuing a trip signal. Obviously, based on the network topology, DG tripped capacity and the instant of DG tripping, the zone interference increases or decreases. This highlights the necessity to enable the protection on transmission side to adaptively balance security versus dependability for handling these unexpected events and save the power system from catastrophic failures. The protection scheme should be able to distinguish such cases from faults and block/unblock tripping signals of vulnerable relays accordingly.

It is worth pointing out that the above-mentioned concern does not extend to conventional generator tripping in the system for two main reasons. Firstly, according to the NERC standard, conventional generators are required to stay connected to the grid throughout almost all the disturbances to maintain the system's synchronization by their turbine-generator inertia [34-35]. They participate in load frequency control (LFC) and automatic governor control (AGC) actions performed by ISOs sending control signals and

set points to the generators in real-time to set their outputs [36]. Secondly, the dynamic planning studies performed by ISOs according to the NERC standard [37] already check the dynamic behavior of the system to be reliable and safe for N-1 contingency cases including each conventional generator tripping. Before a conventional generator is connected and added to the grid, it will be verified that its unintended tripping will not lead to any system instability or cascade event and the required precautions and corrective actions would be planned [37]. The distance protection on transmission side is coordinated for these N-1 contingency cases [31]. However, planning and protection studies for transmission network are based on the network models that do not contain DG protection models, and detailed protection information is not included in the bulk DG planning studies [38-39].

3. PROBLEM FORMULATION

3.1. Dynamic Balance of Protection Dependability and Security

As mentioned before, the problem under consideration is to improve protection reliability under high-impact low-probability events, N-m contingencies, and system resilience consequently. Obviously, it may not be reasonable to expect having protection solutions, e.g. proper settings, developed off-line to cover all the possible N-m contingency cases. Instead, a dynamic trade-off between security and dependability is required as the system goes through events. An improved protection system design must provide inherently dependable and secure operation. The HCP approach [40-41] aims at achieving that goal as discussed in the following.

3.2. Hierarchically Coordinated Protection Concept

HCP concept has been recently proposed in response to a need for implementing a dynamic trade-off between protection security and dependability [40-41]. The basic idea behind this concept is a dynamic balance between dependability and security, which is obtained through predictive, adaptive and corrective relaying actions. This provides flexibility in the protection schemes behavior to handle the uncertainties associated with the protection operation [40-41]. The concept of the three layers of protection (predictive, adaptive, and corrective), is aimed at balancing the dependability vs. security dynamically to prepare for the disruptive events, absorb them, and recover from them with an appropriated relaying action which leads to supporting system resilience consequently.

Historical data and statistics on contingencies such as weather-related disturbances, equipment outages, etc. is employed by the Predictive Protection layer to identify similar

conditions which may lead to the major disturbances in the future. Advanced data analytics may be used by this layer to conduct the analysis. Possible anticipation of disturbance by this layer provides an opportunity of adjusting bias between dependability and security for the protection system by selecting between groups of relay settings as an example. This is in line with the feature of the system resilience where new lessons are absorbed from the past and proper tools and provisions are made for dealing with future similar crisis.

Inherently Adaptive Protection layer, which is based on the learning algorithms from patterns of the features extracted from the real-time system measurements comes next. Numerous system conditions are involved in the learning process to cover the potential scenarios and then the pattern from real-time measurements are compared against those for system's condition identification. This allows maintaining protection dependability and security without the need to outweigh one against the other. Effective adaptive protection is translated into providing robustness, resourcefulness and improving gradual degradation from the system resilience point of view. It provides resourcefulness and robustness by avoiding relay misoperation which may lead to system collapse or cascading failures under disruptive events (high-impact low probability events).

The Corrective Protection layer deals with assessing the correctness of the protection system operation in real time by utilizing a tool to detect relay misoperation. Should a legacy protection scheme operate, this tool is activated immediately after to detect any misoperation and the corrective action as a consequence of that misoperation is initiated as needed to improve resourcefulness from the resilience perspective by avoiding any unnecessary outages as a result of possible relay misoperaiton and managing the

disturbance as it unfolds.

Such protection adjustment approaches may be coordinated in a hierarchical way by implementing the predictive, adaptive and corrective actions simultaneously to assure improved resiliency by avoiding various unwanted relay operations due to a compromised dependability or security.

3.3. HCP-Based Supervised Legacy Transmission Protection

This dissertation aims at utilizing HCP concept to propose a fundamental protection approach which supervises legacy distance protection transmission lines to improve the protection reliability. Figure 8 shows the general block diagram of the proposed fundamental HCP-based approach. The idea is to supervise the operation of the distance relay before it operates, as it gets ready to operate, and immediately after it operates. The legacy distance protection operates as follows:

- The distance relays primary and backup zones are set for a base network topology and anticipated maximum loadings of the lines. Should the apparent impedance trajectory seen by the relay, as a result of local measurement at the relay location, fall within any of its protective zones for the specific duration of the corresponding zone's settings, the relay will issue a trip signal to the breaker to clear the fault.
- As majority of the faults have a temporary nature, such as lightning hits on transmission lines, an automatic reclosing process is put in place to perform reclosing actions after the relay operation. The reclosing attempts take place with specific preset intervals (dead time) between the actions. If the

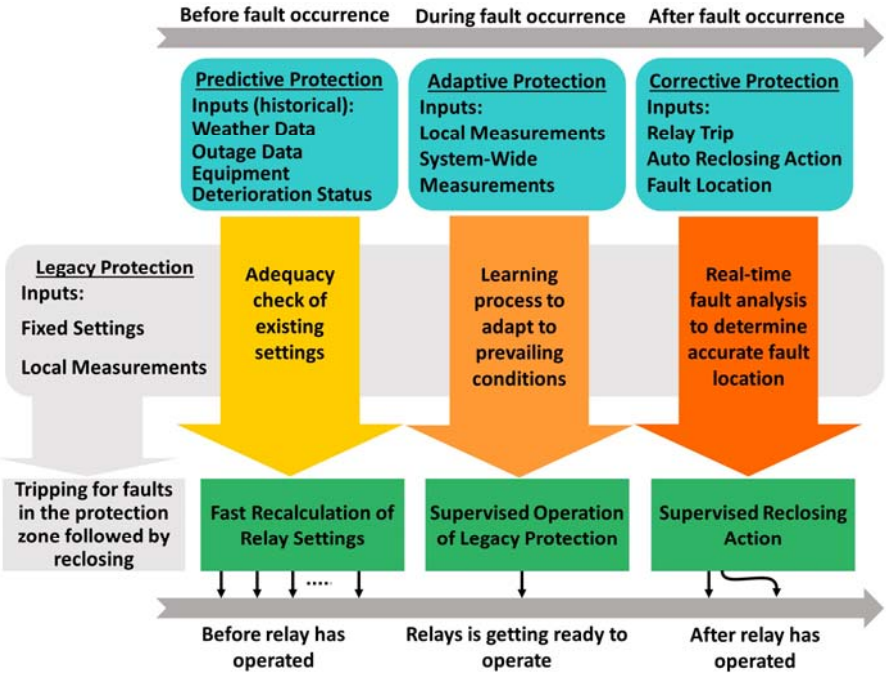

Figure 8. Traditional distance protection supervised by HCP

fault is still identified to exist by the relay after a definite number of reclosing attempts, the relay will issue the final trip signal and lockout any further breaker operation, i.e. the breaker will open the circuit and stay in the open status.

The proposed HCP-based approach intends to supervise the above-mentioned distance operation by:

- Real-time review of the distance settings for an evolving network topology as the predictive protection. The idea is to investigate the settings coordination adequacy before/after a planned/unintended change in the network topology. Vulnerable relay settings are identified, and proper set

of settings are calculated for them to prevent any misoperation of the relay as a consequence of settings coordination inadequacy under the next unpredictable fault happening. Rendering the current network topology is provided via the SCADA system with a resolution in the order of a few minutes.

- Adaptively manage the balance between dependability and security as the contingencies unfold and relay gets ready to operate is the goal of adaptive protection. Machine learning technique is utilized to take online local and system wide measurements as inputs in order to identify proper blocking/unblocking signals in supervising legacy distance relay operation. The learning algorithm can be trained off-line with numerous simulation cases of unintended disruptive events under consideration. Having trained the learning algorithm, the approach is expected to correctly distinguish whether the relay should operate or not under a new unseen case in real-life.
- Should a relay operate, its operation can be investigated immediately via the corrective protection. The idea is to perform a real-time fault analysis in the mean time between the reclosing attempts in order to supervise the reclosing actions and mitigate the consequences of a relay misoperation. For example, if the fault analysis output identifies that the fault is not within the protective zones of the relay which has operated, the reclosing attempts are supervised to avoid any extended extent of outage.

The aggregated hierarchical coordination of the above mentioned three layers of protection, i.e. predictive, adaptive, and corrective, results in a fundamental HCP-based protection scheme to supervise legacy transmission distance protection function and improve protection reliability and system resilience consequently.

4. STATE OF THE ART

As mentioned before, this dissertation is focused on utilizing HCP to supervise legacy transmission protection function. Previous research and efforts which can be considered as related to this area have been surveyed and discussed in the following.

4.1. Automated Distance Setting Calculation

A tedious and time-consuming task for protection engineers is selecting and setting protective relays manually [42-43]. Such a problem is suitable for solution by a computer-aided-design (CAD) approach. Data management techniques are available so that large data sets can be conveniently manipulated and maintained [42-43]. Hence, the tedious manual work can be automated if it is thoroughly understood. But perhaps the most important feature of the CAD approach is the opportunity for the engineer to interact with and guide the solution process with his/her experienced judgement. He/she can exercise options based upon results at intermediate stages in the process to achieve solutions which represent his/her philosophy or take the intuition about the system into consideration.

A major, previous effort to assist protection engineers was oriented toward off-line processing using interactive computer algorithms [44-46]. One of the most recent efforts in this area which has resulted a commercial software package, known as CAPE, could be considered as an effective automated relay setting calculation module which is being used in industry [31]. As mentioned before, this task is still considered as a significantly time-consuming process because of its high computational burden specifically for real-time applications. The ever-improving computation technology calls for revisiting the problem and looking at opportunities for increasing the computation speed. The fast pace of

computation technology improvement can make the ever-desired ability to review the distance settings online which is investigated in this dissertation.

4.2. Machine Learning-Based Protection Schemes

As of late, supervised learning methods (pattern recognition techniques) such as fuzzy logic [47-48], artificial neural network (ANN) [49-54] and support vector machine (SVM) [55-59] have been employed in different areas of power system protection. SVM performance, when compared to the other conventional classifiers the performance of which might suffer from handling huge feature spaces, is not significantly affected by classified vectors dimension [60]. SVMs have the potential to handle very large feature spaces, because the training of SVM is carried out so that the dimension of classified vectors does not have as distinct influence on the performance of SVM as it has on the performance of conventional classifiers. That is why SVM is especially efficient in large classification problems. Furthermore, the great advantage of SVM, which makes it more powerful than other traditional methods based on risk minimization such as ANNs is that it deploys various ideas such as the Vapnik-Chervonenkis theory, statistical learning, maximum margin optimal hyperplane, kernel functions and so on [60]. Also, SVM-based classifiers are claimed to have good generalization properties compared to conventional classifiers, because in training the SVM classier, the so-called structural misclassification risk is to be minimized, whereas traditional classifiers are usually trained so that the empirical risk is minimized [60].

SVM technique has been deployed as a supervised learning method for different power system protection purposes recently. Ravikumar et al. [56] have used SVMs for

post-fault diagnosis purpose as an intelligent tool to identify the faulted line and the distance to the fault. They also have compared SVMs with neural networks for different types of faults on transmission lines. The same authors have deployed SVMs in coordinating the distance relay settings [57]. Samples of apparent impedance seen by the relay during faults are used as SVM input data. In [58], the authors have evaluated and compared various methods of implementing multiclass SVMs in studying the coordination of distance relay settings. Some other studies have used SVM technique for improving protection of transmission lines compensated by series capacitors [59]. They have presented a combined wavelet-SVM technique which uses three-line current samples to detect the faulted zone on a series compensated transmission line.

Deployment of SVM to other applications in the power system protection area is yet to be explored. Employing SVM to address the protection reliability concerns under high penetration of DGs into the power system has not been implemented yet and is studied in this dissertation.

4.3. Real-Time Fault Analysis Approaches

A typical fault analysis tool performs fault detection, classification, and location as a total package. Several efforts in the past have been proposed in this area which are suitable for off-line analysis and not qualify for real-time applications [61-68]. Recent research efforts in this area have accomplished to propose an effective fault analysis approach which is very fast and accurate and proper for the real-time applications [41], [69-70]. In this dissertation the fault analysis approach proposed and improved in [69-70], and [41] is utilized in the corrective layer of the HCP-based protection scheme in order to

supervise the legacy reclosing actions. The fault analysis approach obtains accurate results within a few milliseconds which provides enough margin to be accommodated in the mean time between the first operation of the relay and the last reclosing attempt.

5. PREDICTIVE PROTECTION: AUTOMATED REVIEW OF DISTANCE SETTINGS ADEQUACY*

5.1. Introduction

Operational schemes are being changed in the re-structured power systems. Transmission line switching, mostly for various economic and technical reasons, as well as intermittent output of renewables (when highly penetrated into the system) can be considered as major contradictory changes from the legacy transmission protection standpoint. This is because the setting coordination of the distance relays may be affected due to the change of the network loading levels as well as short circuit values. The tool for real-time review of the distance relays protection coordination adequacy under evolving network topology and power flow is not available yet. Hence an assessment whether a change in the relay settings is needed to maintain the security and dependability of the power system protection at such times is typically not performed.

The focus of this part of the dissertation is to propose a module to investigate the adequacy of the network relay settings for a new (evolving) network topology which takes into the account the current/future power flow data as well and identify the consequent vulnerable relays at selected locations in the transmission system. The proposed module could be used in practice to assess multiple switching impacts on the network relay settings. Furthermore, it enables identifying the relays prone to misoperate under

---

significant changes of renewables output, and power flow consequently, which could be anticipated more precisely using short-term forecasting data. The new calculated settings for the new system topology and power flow are compared with the previous ones to identify the affected relays. The module's output contains the list of the relays whose settings have changed beyond an acceptable margin. It provides the transmission system operators (TSOs) with an extra decision-making tool to assess the adequacy of distance settings for an evolving network topology and power flow so that a proper action can be taken. For example, in the scenario that the operator is provided with a list of switching actions for corrective purposes, e.g. load shedding or cost reduction, he/she is able to assess the switching candidates in regard to their impact on the protection security and dependability when selecting the best option. If the topology has already changed due to maintenance purposes or cascading tripping as a consequence of relay mal-operation, the operator could assess the protection security and dependability for the current topology and take proper action.

5.2. Phase Distance Setting Rules

Utilities, all over the world, follow different rules in setting calculation of the distance relays depending on their approach to operating the network. The setting procedure followed in this study is the same as the default procedure in CAPE [31]. A modern distance relay has several elements which provide many protection functions in a single package. In this study, the focus is on the phase distance elements and mho settings of different zones. There are two ways to calculate the zone settings: one is based on the line ohms only, which is not so practical, and the other, which is used here, is to consider

both the line ohms and the apparent impedance of different fault types seen by the relay [43], Figure 9.

To obtain the initial mho settings, regarding the apparent impedances, three types of fault calculation, as shown in Figure 9, are implemented: a) three-phase fault on remote bus, b) three-phase fault on the next adjacent bus, and c) three-phase line-end fault on the next adjacent line. The maximum torque angle (MTA) is considered the same as the first zone's line angle, i.e., MTA = $\angle Z_l$.

The apparent impedances are checked as follows to make sure they are valid during the setting procedure:

$$z_{rem} = \begin{cases} z_{rem} & \begin{array}{l} |z_{rem}| \le 10 \times |Z_l| \ \& \\ |\angle z_{rem} - \mathrm{MTA}| \le \dfrac{\pi}{4} \end{array} \\ 0 & \text{otherwise} \end{cases} \qquad (1)$$

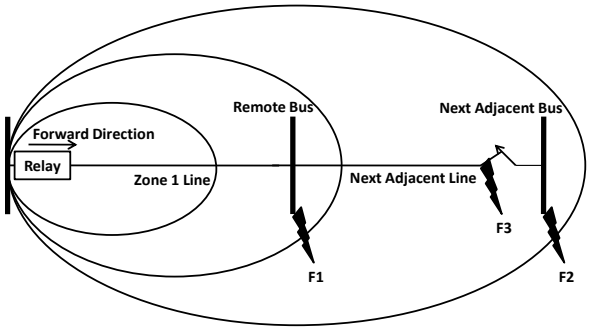

Figure 9. Fault types used for phase distance setting calculation: remote bus fault (F1), next adjacent bus fault (F2), and line-end fault (F3)

$$z_i^{adj}\Big|_{i\in N^{adj}} = \begin{cases} z_i^{adj} & \left|z_i^{adj}\right| \le 10\times\left|Z_l\right| \ \ \& \\ & \left|\angle\, z_i^{adj} - \mathrm{MTA}\right| \le \dfrac{\pi}{4} \\ 0 & \text{otherwise} \end{cases} \quad (2)$$

$$z_{end_i}^{adj}\Big|_{i\in N^{adj}} = \begin{cases} z_{end_i}^{adj} & \left|z_{end_i}^{adj}\right| \le 10\times\left|Z_l\right| \ \ \& \\ & \left|\angle\, z_{end_i}^{adj} - \mathrm{MTA}\right| \le \dfrac{\pi}{4} \\ 0 & \text{otherwise} \end{cases} \quad (3)$$

The phase distance setting rules are as follow:

5.2.1. Zone 1 Setting Rule

$$Z_1 = 0.8\times \mathrm{Z}_l \quad (4)$$

5.2.2. Zone 2 Setting Rule

$$Z_2^l = \max\left\{1.2\times\left|Z_l\right|, \left|Z_l\right| + 0.2\times\left|\min\left(z_{l_i}^{adj}\right)\right|_{i\in N^{adj}}\right\} \quad (5)$$

$$Z_2^{app} = 1.2\times\left|z_{rem}\right| \quad (6)$$

$$Z_2 = \max\left\{Z_2^l, Z_2^{app}\right\} \angle \mathrm{MTA} \quad (7)$$

5.2.3. Zone 3 Setting Rule

$$Z_3^l = 1.2\times\max\left(z_{p_i}^{adj}\right)_{i\in N^{adj}} \quad (8)$$

$$Z_3^{app_{bus}} = 1.1 \times \left| \max\left(z_i^{adj} \right) \right|_{i \in N^{adj}} \quad (9)$$

$$Z_3^{app_{end}} = 1.1 \times \left| \max\left(z_{end_i}^{adj} \right) \right|_{i \in N^{adj}} \quad (10)$$

$$Z_3 = \max\left\{ Z_3^l, Z_3^{app_{bus}}, Z_3^{app_{end}} \right\} \angle \mathrm{MTA} \quad (11)$$

Then, the load encroachment is evaluated for all zones to prevent phase protective relay settings from limiting the transmission system loading capacity while maintaining dependability of the network protection. According to NERC [71], the relay performance should be checked for 150% of the highest seasonal rating of the lines at 0.85 per unit voltage and a power factor angle of 30 degrees:

$$Z_{relay}^{30} = \frac{0.85 \times V_{LL}}{\sqrt{3} \times 1.5 \times I_{rating}} \quad (12)$$

Furthermore, according to setting rules followed by CAPE, the zone settings are checked not to over-reach 20% of the transformer impedance in order not to interfere with the distance relay settings on the lines located after the transformer [31].

5.3. Relay Setting Calculation and Adequacy Check Module

The proposed module contains algorithms which check the adequacy of the existing relay settings for the new system topology after switching. It performs fast relay setting calculation for the new topology and compares the new setting values with the current settings. Figure 10 shows a general flowchart of the proposed setting calculation module.

The critical challenge for actual implementation of this methodology is that the

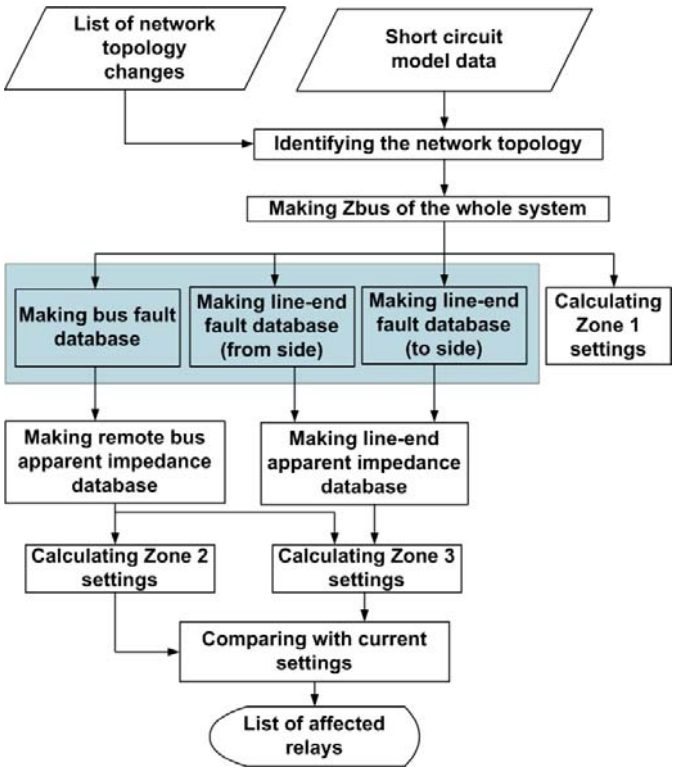

Figure 10. General flowchart of the relay setting calculation module

setting coordination check of distance relays in a transmission operator (TOP) sized system is a significantly time-consuming task and should be automated. Identifying the relays whose settings get affected due to a change of the network short circuit values following a network topology change could be considered as an initial step in conducting automated settings coordination check. Performing the setting coordination check on the affected relays should also be fast enough. As a result, the focus here is also to make the setting calculation process faster by investigating how to reduce the problem size and calculation burden.

5.3.1. Short-Circuit Model Data Preparation

The input for the relay setting calculation module is: 1) short-circuit model data for buses, branches, generators, 2) power flow data, and default relay settings and 3) list of network topology changes. Having recognized the network topology, the module builds up the Z_{bus} for the whole network which is used in fault calculations. Furthermore, a list of network distance relays and their adjacent buses and branches is obtained from the network topology. For each relay the buses and branches on which the bus fault and line-end fault should be implemented respectively to obtain the relay settings are determined. Having identified the required fault calculations for the setting procedure of each distance relay in a network, this method could be implemented on a system with different types of relays without causing an interference with setting calculation of the distance relays in that network. The module could be run for the identified distance relays in the network to assess their settings. Moreover, any exclusive condition such as the type of the relay used at specific points in the network or specific setting procedures (rules) followed by a network operator could be predefined in the module, so the relays are set accordingly.

5.3.2. Fault Database Preparation

During the fault calculations several updates to Z_{bus} are required depending on the fault type. This prevents repetitive and excessive Z_{bus} calculation if not necessary. The sparsity-oriented compensation methods are used to perform updates to Z_{bus} [72]. Z_{bus} should specifically be modified by updating the required column when implementing a line-end fault as assumedly another bus is added to the network. The process of calculating the voltages of all the buses for the case of a line-end fault implemented on the j side of

the line from bus i to bus j, are formulated as follows using branch-oriented compensation method [72]:

$$U_{Nbu\times 1} = \begin{bmatrix} 0 & \dots & \overset{i}{-Y_{ij}} & \dots & 0 \end{bmatrix}^T \tag{13}$$

$$V_{Nbu\times 2} = \begin{bmatrix} 0 & \cdots & 0 & \overset{i}{1} & 0 & \overset{j}{\cdots} & \cdots & \cdots & 0 \\ 0 & \cdots & \cdots & \cdots & 0 & 1 & 0 & \cdots & 0 \end{bmatrix}^T \tag{14}$$

$$\Delta = \begin{bmatrix} 0 & Y_{ij} \\ Y_{ij} & -(Y_{ij} + Y_{sh}) \end{bmatrix} \tag{15}$$

$$\begin{aligned} W &= \left(I_{2\times 2} + \Delta \times V^T \times Z_{bus} \times V \right)^{-1} \times \Delta \\ X &= Z_{bus} \times V \times W \times V^T \times Z_{bus} \\ Z &= \left(Z_{bus} - X \right) \times U \end{aligned} \tag{16}$$

$$Z^{col} = \frac{1}{Y_{ij} + Y_{sh} - U^T \times Z} \begin{bmatrix} Z \\ -1 \end{bmatrix}_{(Nbu+1)\times 1} \tag{17}$$

$$V_n^{post} = V_n^{pre} \left(1 - \frac{Z_{n1}^{col}}{Z_{(Nbu+1)1}^{col}} \right) \quad n \in \{1, \dots, Nbu\} \tag{18}$$

5.4. Implementation of Parallel Computation

The algorithm computation burden mostly relates to the creation of different fault type databases, as shown in the three blocks highlighted in Figure 10. Specifically, line-end fault database preparation for two ends of the line is a very time-consuming task. This is because the power system Z_{bus} is a big order sparse matrix for which operations such as inversion and multiplication shown in (16) to (17), require more computation efforts from

the processor. Each of the fault databases contains the bus voltage and branch current values for the corresponding type of fault. The voltage and current values are then used to calculate the associate apparent impedances. To improve the calculation speed, parallel computation could be performed on the three fault types calculation independently. Figure 11 shows the general flowchart of implementing parallel computation for N tasks each of which might contain several sub-tasks. For the parallel computation to be implemented the tasks should be independent from each other, i.e., there should be no flow of data required between the tasks for each of them to be completed. In that case, all the tasks could be submitted to a group of workers (computing nodes) called pool of workers. Each worker might include several processing cores. The access to input data is provided

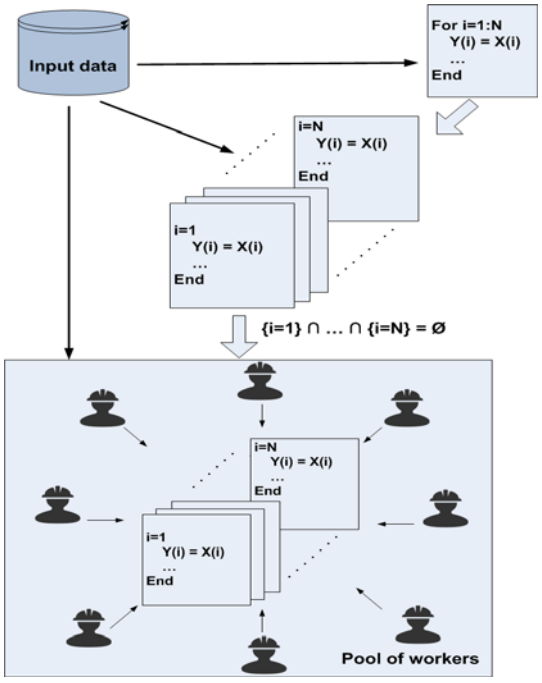

Figure 11. General implementation of parallel computation for N tasks

for all the workers so they can use the same input data. However, the worker does not need any data obtained by other tasks.

Now, as an example, let's discuss how the line-end fault database preparation could be parallelized. Considering to-end of the lines, the goal is to obtain the voltages of all the buses for the faults implemented on all the to-ends of the lines. In other words, (13) to (17) should be calculated for $i = 1{:}Nbr$. As it could be understood from these equations, they could be conducted for branch n completely independent from those of branch m. For each implemented fault, the voltage of all the buses could be calculated and stored separately. This allows implementation of the parallel computation. The same process could be implemented for the from-end of the lines and also for the remote bus fault calculations. The latter could be conducted much faster as no change to Z_{bus} is required to implement it. For a fault implemented on bus n, Z_{col} is simply the nth column of Z_{bus} and there is no need to conduct (16) to (17). The network Z_{bus} is the only common data fed into the three blocks. Having the voltages at both ends of the branches corresponding to each fault case together with their impedances, the branches currents could be easily calculated.

5.5. Distance-of-Impact (DoI) Concept

For the setting calculation process to be practical for real-time applications on real-life networks, the calculation burden and corresponding time should be reduced further. The idea is to avoid the redundant calculations for assessing the adequacy of the settings following a network topology change. Thus far, the proposed setting calculation module is assumed to run the setting calculation for all of the relays in the network for a topology change to identify the relays which settings have been affected. However, the fundamental

concept of network Z_{bus}, which is the core element of the distance settings calculations as mentioned before, brings the idea into mind that the impact of a change in the network topology on the short circuit values (voltages and currents) has to be limited to a certain electrical distance from the location of the network topology change and it should fade away for farther points in the network. This has been explained further in detail in the following.

Network Z_{bus} is a symmetrical full matrix which can be obtained by getting the inverse of the Y_{bus} which is a symmetrical sparse matrix. The element Z_{ik} of the Z_{bus} matrix can be interpreted as the change in the voltage of bus *i* (ΔV_i) caused by injecting current into bus *k* (ΔI_k). Therefore, if ΔI_k is injected in bus k, the change of voltage on the network buses can be obtained as follows:

$$\begin{bmatrix} \Delta V_1 \\ \Delta V_2 \\ \vdots \\ \Delta V_k \\ \vdots \\ \Delta V_N \end{bmatrix} = \begin{bmatrix} Z_{11} & Z_{12} & \dots & Z_{1k} & \dots & Z_{1N} \\ Z_{21} & Z_{22} & \dots & Z_{2k} & \dots & Z_{2N} \\ \vdots & \vdots & \ddots & \vdots & \ddots & \vdots \\ Z_{k1} & Z_{k2} & \dots & Z_{kk} & \dots & Z_{kN} \\ \vdots & \vdots & \ddots & \vdots & \ddots & \vdots \\ Z_{N1} & Z_{N2} & \dots & Z_{Nk} & \dots & Z_{NN} \end{bmatrix} \begin{bmatrix} 0 \\ 0 \\ \vdots \\ \Delta I_k \\ \vdots \\ 0 \end{bmatrix}$$

Which results in:

$$\begin{bmatrix} \Delta V_1 \\ \Delta V_2 \\ \vdots \\ \Delta V_k \\ \vdots \\ \Delta V_N \end{bmatrix} = \begin{bmatrix} Z_{1k} \\ Z_{2k} \\ \vdots \\ Z_{kk} \\ \vdots \\ Z_{Nk} \end{bmatrix} \Delta I_k$$

This interpretation from the network Z_{bus} is specifically useful for power system contingency analysis applications. In this study, the focus is on the impact of a change in the network topology, adding/removing a line from the grid as an example, on the network

short circuit values. When considering line additions to or removals from an existing system, it is not always necessary to build a new Z_{bus} or to calculate new triangular factors of Y_{bus} especially if the only interest is to establish the impact of the changes on the existing bus voltages and line currents. An alternative procedure is to consider the injection of compensating currents into the existing system to account for the effect of the line changes. To illustrate the basic concept, let us consider removing a line with the impedance of Z_a from an existing system with known Z_{bus}.

Assume the impedance Z_a is connected between buses m-n of the system. The bus voltages $V_1, V_2, \ldots, V_N$ are known to be produced in the original system (before removing Z_a) by current injections $I_1, I_2, \ldots, I_N$ which are fixed in value as shown in Fig. 12. On a per-phase basis, the bus impedance equations for the original system are then given by:

$$\begin{bmatrix} V_1 \\ \vdots \\ V_m \\ V_n \\ \vdots \\ V_N \end{bmatrix} = \begin{bmatrix} Z_{11} & \cdots & Z_{1m} & Z_{1n} & \cdots & Z_{1N} \\ \vdots & \cdots & \vdots & \vdots & \cdots & \vdots \\ Z_{m1} & \ddots & Z_{mm} & Z_{mn} & \ddots & Z_{mN} \\ Z_{n1} & \cdots & Z_{nm} & Z_{nn} & \cdots & Z_{nN} \\ \vdots & \ddots & \vdots & \vdots & \ddots & \vdots \\ Z_{N1} & \cdots & Z_{Nm} & Z_{Nn} & \cdots & Z_{NN} \end{bmatrix} \begin{bmatrix} I_1 \\ \vdots \\ I_m \\ I_n \\ \vdots \\ I_N \end{bmatrix}$$

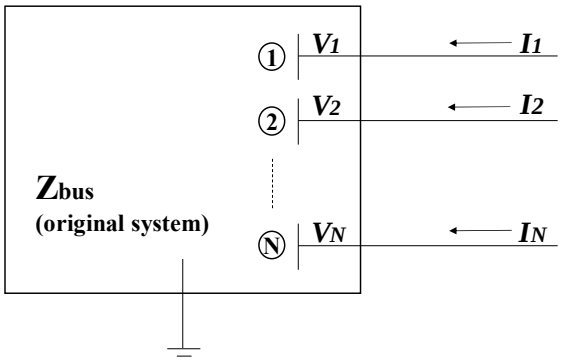

Figure 12. Original system with voltages $V_1, V_2, \ldots, V_N$ as a result of the current injection $I_1, I_2, \ldots, I_N$

The goal is to determine the changes in the bus voltages due to removing the branch Z_a. The line removal is equivalent to injecting opposite currents, compared to existing current injections at both ends of the line, as shown in Fig. 13. Therefore, the ΔV on the network buses as a result of the line removal can be obtained from:

$$\begin{bmatrix} \Delta V_1 \\ \vdots \\ \Delta V_m \\ \Delta V_n \\ \vdots \\ \Delta V_N \end{bmatrix} = \begin{bmatrix} Z_{11} & \dots & Z_{1m} & Z_{1n} & \dots & Z_{1N} \\ \vdots & \dots & \vdots & \vdots & \dots & \vdots \\ Z_{m1} & \ddots & Z_{mm} & Z_{mn} & \ddots & Z_{mN} \\ Z_{n1} & \dots & Z_{nm} & Z_{nn} & \dots & Z_{nN} \\ \vdots & \ddots & \vdots & \vdots & \ddots & \vdots \\ Z_{N1} & \dots & Z_{Nm} & Z_{Nn} & \dots & Z_{NN} \end{bmatrix} \begin{bmatrix} 0 \\ \vdots \\ I_a \\ -I_a \\ \vdots \\ 0 \end{bmatrix}$$

And in a simpler form:

$$\begin{bmatrix} \Delta V_1 \\ \vdots \\ \Delta V_m \\ \Delta V_n \\ \vdots \\ \Delta V_N \end{bmatrix} = \begin{bmatrix} Z_{1m} - Z_{1n} \\ \vdots \\ Z_{mm} - Z_{mn} \\ Z_{nm} - Z_{nn} \\ \vdots \\ Z_{Nm} - Z_{Nn} \end{bmatrix} I_a$$

Now, let us picture what mentioned above on an example network (IEEE 118-bus

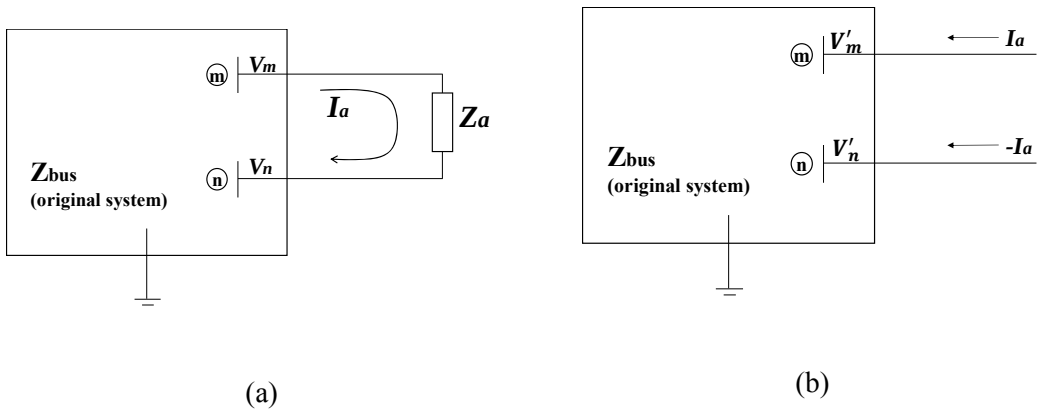

(a) (b)

Figure 13. Original system of Fig.12; (a) having Z_a in the network, (b) removing Z_a by injecting corresponding compensation currents at both ends

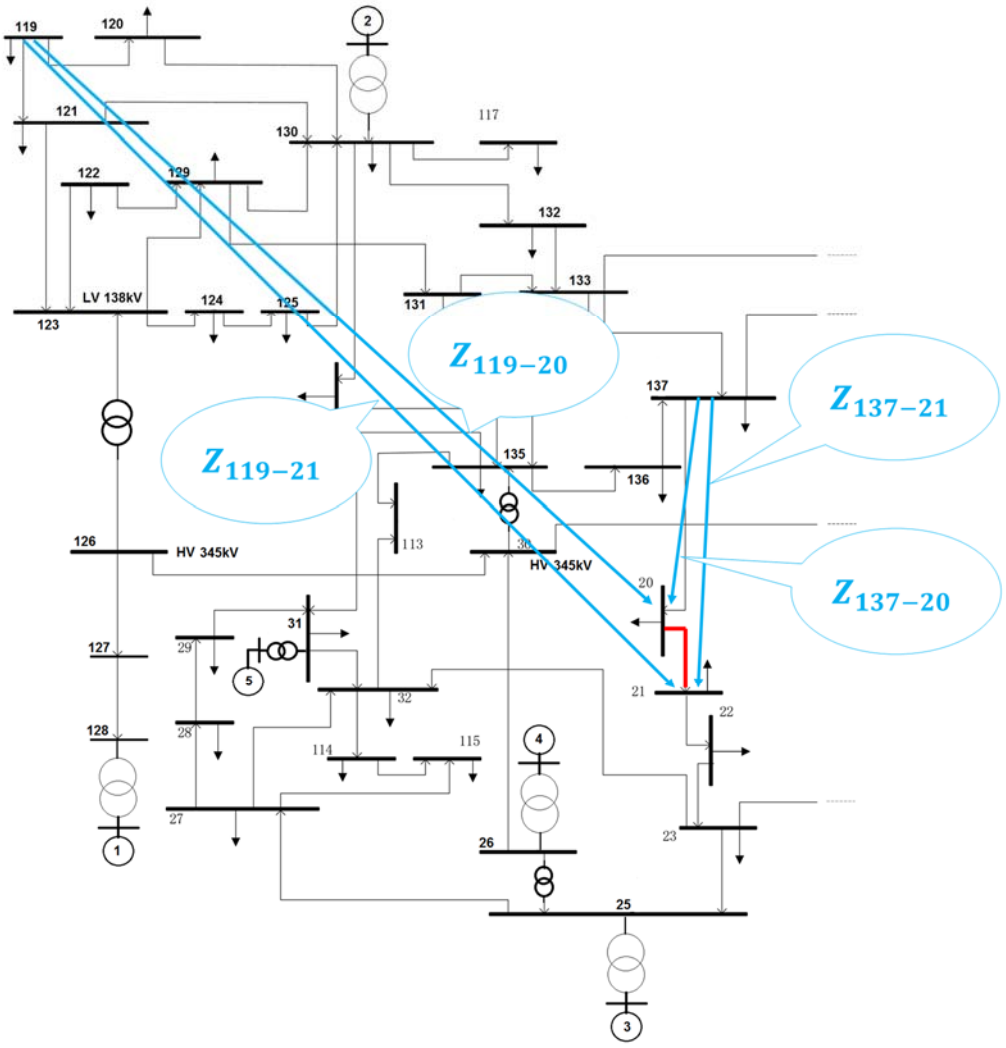

Figure 14. A part of IEEE 118-bus system

system; buses are renumbered for calculation purposes) to better understand the situation, Fig. 14. It is assumed that the line 20-21 is removed from the network and we want to estimate the impact of the branch removal on the voltage of the two buses 119 and 137 which are considered electrically close and far from the ends of the line 20-21 respectively. The difference of $Z_{119\text{-}20}$ and $Z_{119\text{-}21}$ (i.e. $Z_{119\text{-}20} - Z_{119\text{-}21}$) is a smaller value compared to

the difference of $Z_{137\text{-}20}$ and $Z_{137\text{-}21}$ (i.e. $Z_{137\text{-}20} - Z_{137\text{-}21}$); 0.002pu and 0.024pu respectively for this network. According to the above equations, this means a lower ΔV on the bus 119 compared to that of bus 137 as a result of the branch removal. However, the ΔV on both buses depend on the system interconnectivity and the pre-removal line current magnitude on branch 20-21; therefore, identifying the electrical distance from the topology change beyond which the impact of the topology change on the bus voltages can be ignored is case specific for each network.

For this purpose, we have investigated the distance-of-impact (DoI) concept, which determines how far from the line that experiences a switching action one can expect the relay settings to be affected. This has been verified from conducting numerous simulations on both the 118-bus and Alberta transmission operator systems as will be discussed in the next Section. In the case that the switching actions impact on the relay settings is limited to a certain electrical distance from the switching location, the calculations are then focused on the portion of the network within that distance. Figure 15 illustrates an example to clarify the DoI concept. For the switched transmission line a-b, the DoI of one includes the buses c to f with their corresponding branches and relays, and DoI of two includes

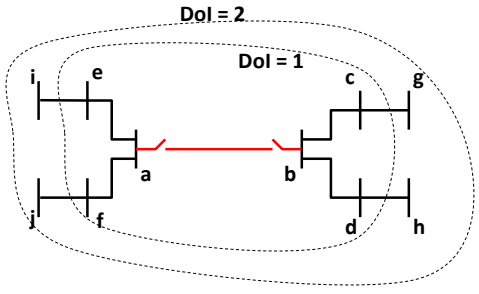

Figure 15. Illustrating the concept of DoI

those of the buses c to j.

5.6. Case Study

The performance of the proposed module is tested on the synthetic IEEE 118-bus [73] and real-life Alberta transmission operator system [74]. The actual calculated relay setting values are verified by comparing them with the output of CAPE commercial package used in the project reports submitted to ARPA-E, U.S. Department of Energy [75]. The relays are assumed to be set only in the forward direction as shown in Figure 9. The transmission lines do not have mutual coupling and transformer protection is neglected for the sake of simplicity. In general, the impact of mutual coupling is limited to the relays on the lines with such feature and could be modeled by proper changes to the network Z_{bus} so it does not harm the effectiveness and generality of the proposed approach and it does not introduce a significant additional computational burden. The distance protection is not the best option for transformer protection and it is assumed that transformers are normally protected by differential relays.

5.6.1. Sensitivity Analysis

In the first step of the simulations, a sensitivity analysis to investigate the impact on the network relay settings by N-2 contingencies with 2 lines switched out has been done using IEEE 118-bus test system. The N-2 contingencies are chosen to be studied because of two reasons: 1) the number of cases to be investigated and 2) they are practical switching scenarios in today's power systems. Conducting each case is significantly fast as the size of the system is rather small. All N-2 contingencies for which the power flow solution converges have been considered (13945 cases in total). A sensitivity analysis is used to

Table 1. Results of sensitivity analysis on the IEEE 118 bus test system

Rank	Critical Relays		Critical N-2 Contingency Cases		Critical Lines	
	Relay	Participation Ratio (%)	Lines (from-to)	No. of Affected Relays	Lines (from-to)	Participation Ratio (%)
1	$R_{98\text{-}80}$	18.32	60-61 & 82-83	21	82-83	35.74
2	$R_{57\text{-}56}$	16.9	60-61 & 82-96	18	94-100	27.58
3	$R_{58\text{-}56}$	12.35	54-56 & 82-83	18	82-96	26.45
4	$R_{16\text{-}17}$	10.24	49-51 & 82-83	18	60-61	23.13
5	$R_{70\text{-}24}$	10.2	31-32 & 82-83	18	11-12	19.42
6	$R_{62\text{-}60}$	10.13	15-19 & 82-83	18	31-32	19.34
7	$R_{54\text{-}55}$	10.06	11-12 & 82-83	18	49-51	18.54
8	$R_{105\text{-}106}$	9.98	82-83 & 100-106	17	54-56	18.25
9	$R_{59\text{-}54}$	9.76	82-83 &100-104	17	100-103	17.56
10	$R_{17\text{-}15}$	9.72	60-61 & 94-100	17	100-104	17.52

detect and rank the probable system protection vulnerabilities following a network topology change leading to N-2 contingency.

Multiple results from the sensitivity analysis conducted on IEEE 118-bus system could be seen in Table 1. The relays whose settings change for a greater number of N-2 contingencies are identified as vulnerable points in the network protection. A relay is considered being affected if its zone 2 or zone 3 experiences a change beyond 5% of the

base network settings. Zone 1 is not a concern as it is only based on the line impedance. Top 10 vulnerable points (critical relays) in the network protection following N-2 contingency cases are ranked in Table 1 based on the number of N-2 contingency cases which affect them. The participation ratio for a relay means the ratio of the number of N-2 contingency cases which have affected the relay to the total number of contingency cases. Top 10 N-2 contingency cases according to their impacts on the network relay settings, and number of affected relays, are also shown in Table 1. The lines participating in the majority of the N-2 contingency cases with significant impacts on the relay settings could also be identified from the sensitivity analysis. Table 1 shows top 10 of such critical lines.

Table 2. N-2 Contingency cases affecting major relay settings

Rank	Lines (from-to)	No. of Affected Relays
1	89-91 & 579-585	29
2	420-865 & 666-1691	29
3	420-865 & 1318-1344	25
4	207-590 & 666-1200	23
5	208-581 & 242-253	23
6	35-331 & 167-737	22
7	297-483 & 669-677	22
8	35-331 & 666-1670	22
9	152-988 & 1431-1484	22
10	63-821 & 136-514	21

In the second step of the simulations, the same sensitivity analysis was conducted for 1000 N-2 contingency cases on Alberta transmission operator system. The top 10 N-2 contingency cases with major impact on the relay settings are shown in Table 2. The size of this system is rather big (2585 buses and 2970 branches) and the relay setting calculation process is time-consuming, specifically the process of creating and updating the line-end fault databases. The parallel computation and supercomputing facilities have been deployed to conduct the contingency cases as will be discussed in the next section.

5.6.2. The Role of Parallelization

Parallel computation technique is implemented to increase the calculation speed. For this purpose, Texas A&M University supercomputing facility [76] with the access to the maximum of 32 workers (nodes) of the facility to conduct the simulations has been employed.

The simulation time to run the setting module for each N-2 contingency case of 118-bus system is insignificant already (less than a second) when using only one processing node of supercomputing facilities even without employing parallel computation. Therefore, to show the effectiveness of the parallel computation technique in improving the calculation speed on IEEE 118-bus test system, it is deployed in conducting all the contingency cases (13945 cases) together when having access to different numbers of workers. On the other hand, running the setting calculation module for each contingency case of the real sized Alberta transmission operator system is significantly time consuming. The improvements from parallel computation could be seen when implemented on even one contingency case. For Alberta system, the setting module

is run for the case ranked first in Table 2 having access to different numbers of workers. Figure 16 (a) and (b) show how parallel computation could significantly improve the module calculation speed based on the available numbers of workers for IEEE 118-bus system and Alberta system respectively. In Figure 16, one worker represents running the module without parallelization. These results provide a perspective how parallel

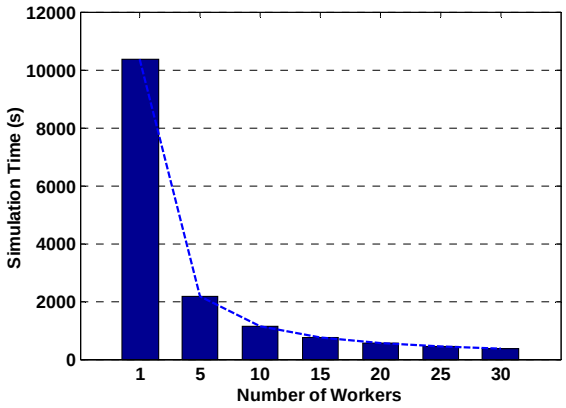

(a)

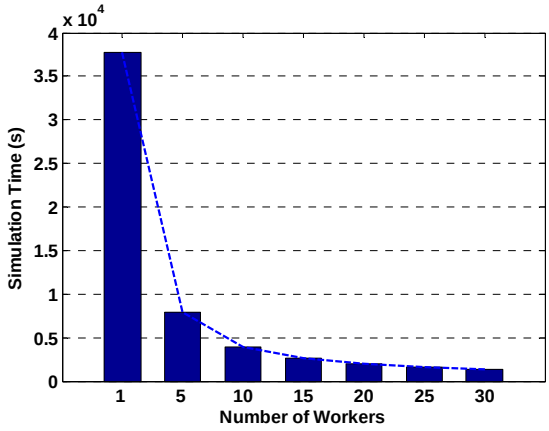

(b)

Figure 16. Simulation time based on the number of workers; (a) Running the module for all the N-2 contingency cases together in IEEE 118-bus system; (b) Running the module for the contingency case ranked 1st in Table 2 for Alberta system

computation benefits escalate especially when the module is conducted on a TOP-sized network. While the cost of supercomputing facility may be prohibitive for the control room setting today, the simulation time could be improved to a desired level just using the ordinary high-end control room computers. With the pace of the technology development, the use of the supercomputers in the control room may be feasible in the near future.

5.6.3. The Role of Distance-of-Impact

Another focus of the sensitivity analysis was to search for the DoI of the switching actions. For this purpose, a search space of the branches starting from the ones adjacent to both ends of the line participating in the switching action is created. The search space grows based on the network connectivity graph till it covers all the affected relays on the network branches. For IEEE 118-bus test system, it was observed that the impact of N-2 contingency cases is limited to the relays on the branches within DoI=3 of the switching action as it could be seen for the top 10 cases in Table 3. Figure 17 shows one-line diagram of IEEE 118-bus test system for which the switching actions 60-61 and 82-83, the contingency case ranked first in Table 1, are highlighted in red. The neighboring branches up to DoI of three are highlighted in blue and as it could be seen the affected relays, which are shown by red arrows, are within the DoI. Using DoI concept, the relays for which the

Table 3. Distance of impact for top 10 cases in both systems

Rank		1	2	3	4	5	6	7	8	9	10
DoI	IEEE 118-bus system	3	2	3	3	3	3	3	2	2	2
	Alberta TOP system	5	5	5	3	4	5	5	5	4	4

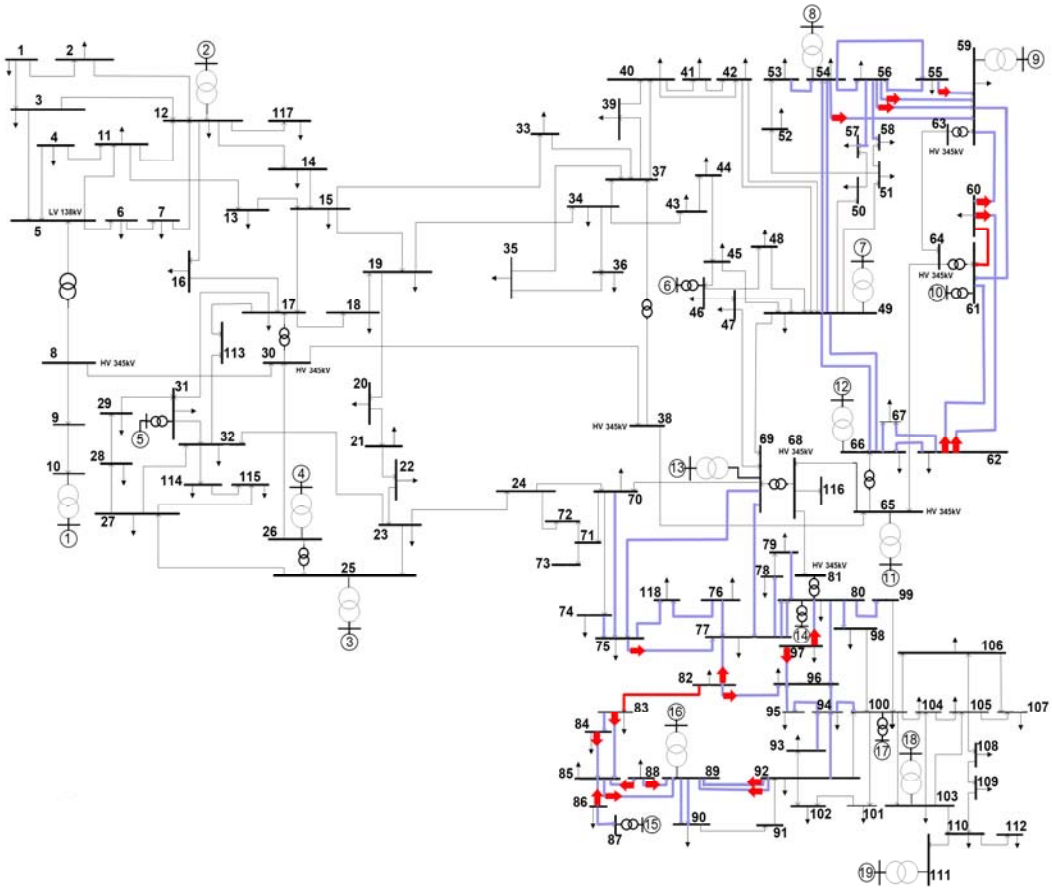

Figure 17. One-line diagram of IEEE 118-bus test system

short circuit values should be updated are the ones within the DoI of the switching action leading to a significant reduction in computational burden.

The sensitivity analysis for the contingency cases in Alberta transmission operator system points the maximum of DoI to be 5 as shown in Table 3 for the previously obtained top 10 contingency cases. The number of buses and branches within DoI = 3 and DoI = 5 for the top 10 cases in IEEE 118-bus and Alberta transmission operator systems

respectively are shown in Table 4. The number of relays which settings are to be checked is two times the number of branches in DoI. As mentioned before, creating and updating the line-end fault database is the most time-consuming part of the setting calculation process. Following the network topology change, the line-end fault values for the relays within DoI should be updated. Figure 18 (a) and (b) shows the simulation time for the cases ranked first in Tables 1 and 2 respectively based on different number of implemented line-end faults to obtain the updated values. Different numbers of line-end faults are obtained based on the number of relays within the DoI as it increases from the switching

Table 4. Portion of the network within DoI for both systems

Rank	IEEE 118-bus (DoI=3)		Alberta (DoI=5)	
	No. of Buses	No. of Branches	No. of Buses	No. of Branches
1	56	113	239	420
2	60	120	310	569
3	65	122	242	467
4	73	133	303	542
5	64	131	168	325
6	72	142	236	447
7	59	120	198	348
8	50	94	176	305
9	50	94	364	660
10	59	114	229	407

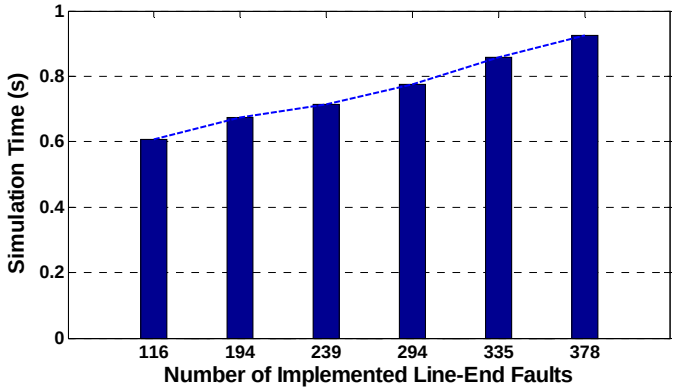

(a)

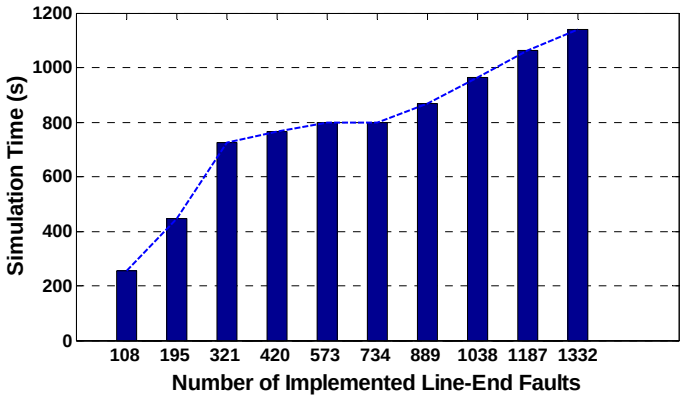

(b)

Figure 18. Simulation time based on the required number of line-end faults; (a) Case ranked 1st in Table I in IEEE 118-bus system; (b) Case ranked 1st in Table I in Alberta transmission operator system

action location.

These simulations are conducted while deploying 1 worker for IEEE 118-bus system and 30 workers for Alberta system. As it could be seen from Figure 15, simulation time could be significantly reduced depending on the required number of line-end fault simulations especially in a real sized system.

Considering the DoI, the calculations could be done exclusively for the relays in the portion of the network within the distance. This leads to significant time savings in simulations as shown in Figure 19 (a) and (b). The calculation time for 10 cases of Tables 1 and 2 could be compared respectively between 2 scenarios: 1) running the setting

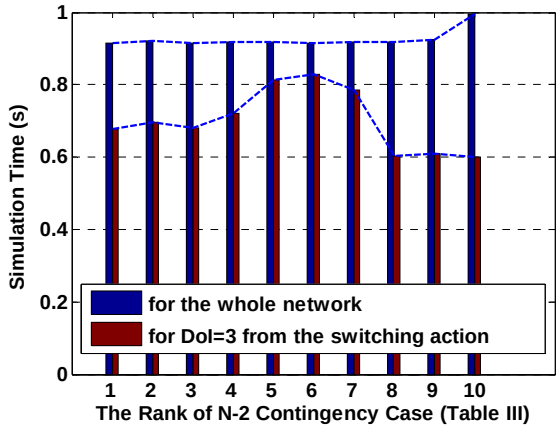

(a)

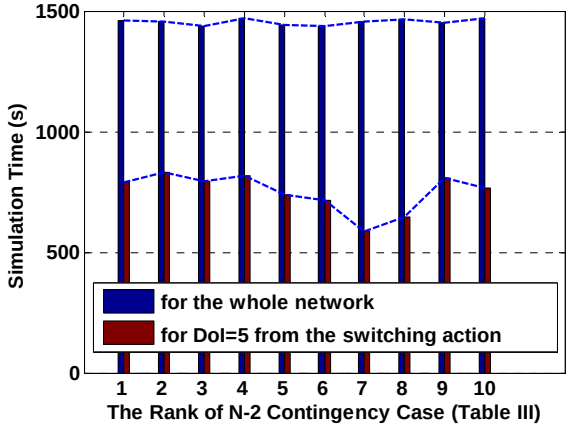

(b)

Figure 19. Simulation time comparison between with and without implementing DoI; (a) Top 10 cases of IEEE 118-bus system; (b) Top 10 cases of Alberta transmission operator system

calculation module for the whole system and 2) doing it for the portion of the system within DoI = 3 for 118-bus system and DoI = 5 for Alberta transmission operator system. The parallel computation has been deployed in both scenarios for Alberta system. In the first scenario, the simulation time for all cases is almost the same while in the second scenario it changes based on the network connectivity graph. As it could be seen from Figure 19, the calculation time has been reduced significantly and real-time identification of vulnerable relays following a network topology change becomes more practical.

5.7. Conclusions

The contributions of this part of the research are as follows:

- The proposed algorithm allows a novel way of setting calculation and evaluation under changing network topology.
- The proposed parallel computation technique significantly reduces the computation time and makes the approach applicable for real-time analysis.
- The proposed calculation module follows the same relay setting procedure as CAPE commercial package and is tested and verified on real-sized Alberta transmission operator systems.
- The proposed distance of impact (DoI) metric is realized to handle numerous cases of network topology changes in the form of N-2 contingencies, which significantly reduces the computation burden.

The proposed decision-making tool can allow the utility staff to assess the impact of multiple switching actions and network topology changes on network protection security and dependability leading to a proper setting coordination action.

6. ADAPTIVE PROTECTION: SVM-BASED PROTECTION SCHEME*

6.1. Introduction

In today's modern power systems, DGs are growing rapidly based on economic and environmental incentives [77]. They are required to follow standards for connecting to the grid and have control and protection measures on their interconnections to be able to disconnect from the distribution grid in case of an inadvertent islanding [78-83]. Inadvertent islanding is called to the situation when DG continues energizing a portion of the system, e.g. the feeder that it is connected to, while being disconnected from the main grid [84]. The duration and probability of an inadvertent island occurrence must be minimized for several reasons such as mitigating power quality, maintaining protection settings, addressing auto reclosing issues, and most importantly ensuring the staff safety [84]. Several anti-islanding protection schemes which are mainly categorized into communication based and local measurement-based methods have been proposed and developed based on this necessity [84-85]. Since deploying communication-based methods, known as transfer trip, is not cost effective for widespread use, the local measurement-based methods are commonly used for anti-islanding protection purposes at the distribution level [84]. Generally, the local measurement-based methods are divided into active and passive ones for which the set of protection schemes consist of under and over frequency and voltage relays [84-85].

On the other hand, sensitive protection schemes being in charge of tripping DGs could act as a threat to the upstream network's post disturbance response as the DG penetration grows in the system. This is because of their probable maloperation as a consequence of a severe disturbance happening upstream which could trigger unintended bulk DG tripping on the distribution side and impose extra stress on the system.

One critical consequence of the additional imposed load flow stress on the upstream network as a result of the unintended bulk DG tripping is the probable unforeseen interference with the conventional distance protection [28-29] as investigated in more detail in this part of the dissertation. According to what is mentioned thus far, it could be concluded that it is necessary to make sure the dependability and security of the protection on the transmission side is not affected by such unintended events to prevent damage extension from distribution to the bulk power system. Although the impacts of unintended DG tripping on transmission protection coordination has been brought up in the literature [28-29], no protection scheme has been specifically proposed against undesirable tripping of distance relays under such circumstances. In this part of the research, a novel SVM-based scheme is proposed to maintain the transmission protection security and dependability under unintended bulk DG tripping on the distribution side, which may occur as a result of maloperation of the deployed anti-islanding schemes. SVM machine learning method has been chosen here in order to handle large feature space which is the nature of the problem under consideration as well as to capture the dynamic interaction between the feature values, i.e. system measurements such as voltages, currents, etc., corresponding to system dynamic behavior under various events, e.g. faults, unintended

DG tripping, etc.

The proposed SVM-based scheme enables the vulnerable distance relays (target relays), the backup settings (second or third zones) of which might get affected under unintended DG tripping events, to distinguish such events from faults and block/un-block the relay operation correspondingly. The proposed setting adequacy check module discussed in Section 5 is used to identify the target relays in the test system. Selective system wide measurements obtained by PMUs in addition to local measurements at the distance relay location are used to improve the proposed scheme accuracy. The scheme's robustness against PMU data loss or unavailability as well as cost-wise use of system wide measurement technology has been taken into consideration in the proposed method. The SVM is trained such that it distinguishes the faults from the DG tripping cases and acts as the supervisory control of the distance backup protection. In the case of unintended DG tripping interference with the distance relay setting coordination, the proposed scheme blocks the conventional trip signal resulting from the distance mho elements' pickup and prevents any follow on the distance relay misoperation. Furthermore, unlike conventional blocking schemes, the proposed method is able not only to block the relay operation due to DG tripping interference, but also to detect a fault during the blocking period and unblock the relay correspondingly. The proposed scheme is easily and quickly trainable for various possible scenarios of system operation in practice and gives significant selectivity. Moreover, it could be considered as another complementary application of SVM along with previously proposed ones to obtain a comprehensive supervisory control protection scheme and improve the protection security and dependability.

6.2. Background

The anti-islanding protection schemes are responsible for detaching the DGs from the grid in case of an inadvertent islanding. The basic idea is sensing the voltage and frequency deviations and checking them against the threshold values to come up with the control action. The critical need to prevent islanding occurrence, especially in order to guarantee the personnel's safety, along with some probable hard-to-detect cases of islanding [29] drives the anti-islanding protection control and measures to be sensitive enough to detect the islanding cases. On the other hand, these sensitive protection measures could affect the DG output unnecessarily under certain circumstances and aggravate the power system dynamic behavior during or after disturbances. Under frequency and voltage sensitivities are two important indicators of such conditions. The former corresponds to a generation-load mismatch situation which may trigger bulk DG tripping, which deteriorates the situation further. Such cases of unintended DG tripping could be mitigated by taking proper immediate load shedding actions, which is not the focus of this study.

The voltage sag caused by severe disturbances such as 3-phase faults at the transmission side could propagate to the distribution level and interfere with DG's under-voltage protection measures, which may lead to unintended DG tripping. This might not raise any significant issue if the existing DG in the system is of small scale and the system is well-designed to handle that. However, in case of high penetration of DG in the distribution network, connected to upstream through a point of common coupling (PCC), the large-scale tripping of the DG units puts an extra power flow burden on the transmission lines. As a result, protection coordination of distance relays' backup

protection zones on transmission side might get affected. The sudden power flow increase to compensate the lack of DG in the system which is already under stress from previous disturbance could initiate distance relay miss-operation and lead to cascade events. Other disturbances such as major switching actions (lines or generators tripping) could also lead to significant voltage deviations which might be potential cause of DG tripping.

Figure 20 helps to illustrate the problem under consideration. Anti-islanding protection scheme makes sure that the DG connected to a feeder (Feeder 1-Feeder 4) would trip if the feeder's source-side circuit breaker (CB1-CB4) opens, usually as a result of a fault on the feeder. A short-circuit happens on the line 9-6 and it is tripped to clear the fault. The voltage drop and deviations as a result of fault occurrence and clearing event

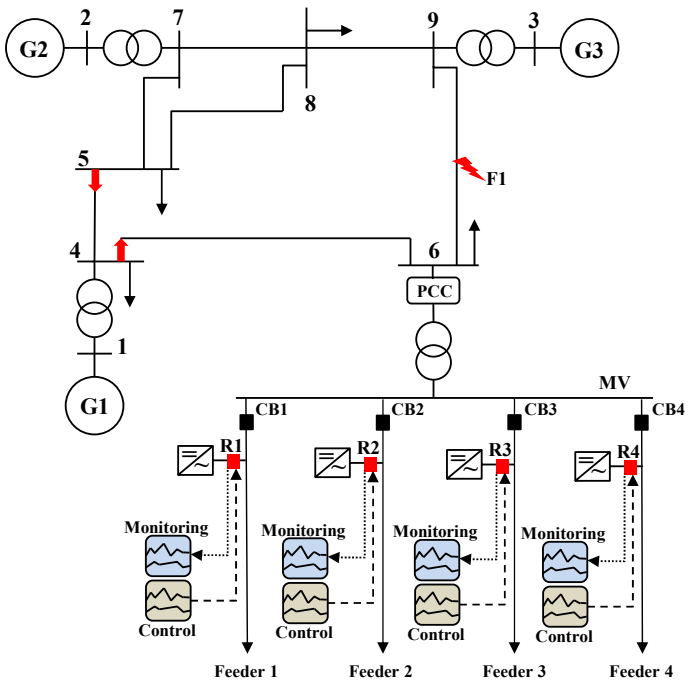

Figure 20. Possible scenario of unintended bulk DG tripping as a consequence of under voltage trip sensitivity

propagates to the distribution side. Assuming the DGs are tripped mistakenly by their anti-islanding protection systems, a sudden power flow increase is imposed on the lines 5-4 and 4-6 to compensate for the lack of DGs while the system is still under the stress of the previous disturbance. This might cause an interference with setting coordination of distance relays on these lines (marked by red arrows) as a result of unexpected dynamic change of the impedance trajectory and trigger their miss-operation, isolation of buses 4 and 6, and lead to the total system collapse consequently. It should be noted that, this is just a simple graphical example to help picturing the problem tentatively; of course, various parameters including the dynamic behavior of the system, impedances of the lines, the settings of the distance relays, the capacity and instant of the tripped DG, loadability of the lines, etc. are important in determining whether it would cause the distance relays misoperation or not. A real demonstration of this scenario on New-England 39-bus system will be presented in the case study Section.

The problem described above highlights the necessity to manage the protection on transmission side to be able to come into the action and act quickly in case of an unintended operation by anti-islanding schemes on the distribution side to save the upstream network. It should be able to distinguish such cases from faults and block/unblock tripping signals of vulnerable relays' backup protective zones accordingly.

6.3. SVM Technique

6.3.1. Brief Overview

SVM is a relatively new and promising machine learning technique to be deployed as a pattern recognition and classification tool. It is based on the statistical learning theory

for ‘distribution-free learning from data’ proposed by Vapnik [86]. In this method, first, the input data is mapped into feature space which is a high-dimensional dot product space and then it is classified through a hyper-plane. Using optimization theory, the maximum separation is obtained by the optimal hyper-plane.

Suppose $x_i \in R^n$ and $i \in \{1, \ldots, l\}$ is the input data including l data points which could be classified into two classes, class I and class II, with the labels of $y_i = 1$, and $y_i = -1$. The goal of SVM linear separation is to identify the optimal hyper-plane which creates the maximum separation between the data points regarding their classes. For the above-mentioned classes, such a separating hyper-plane could be achieved by finding out proper values for w, vector of weights, and b, biased scalar, in the following equation:

$$f(x) = w^T x + b = 0 \tag{1}$$

For a separating hyper-plane:

$$\begin{cases} f(x_i) \geq 1 & \text{if } y_i = +1 \\ f(x_i) \leq -1 & \text{if } y_i = -1 \end{cases} \tag{2}$$

Therefore, $y_i f(x_i) = y_i (w^T x_i + b) \geq 1$ for $i = 1, \ldots, l$. From the geometry, it is found that: $m = 2\|w\|^{-1}$ in which m represents the separation margin. So, maximizing m which means better generalization capability of SVM requires to minimize $\|w\|$. Hence, finding the optimal hyper-plane could be formulated as the following convex optimization problem:

$$\begin{aligned} &\min \ \frac{1}{2} w^T w \\ &s.t. \quad y_i (w^T x_i + b) \geq 1 \quad \forall i \end{aligned} \tag{3}$$

There exists no hyper-plane if it is not possible to separate data linearly; i.e., the constraints in (2) cannot be satisfied all together. In such cases, a penalty factor C and slack variables ξ_i are deployed to introduce a soft margin. The optimization problem then changes to:

$$\begin{aligned} &\min \ \frac{1}{2} w^T w + C \sum_{i=1}^{l} \xi_i \\ &s.t. \quad y_i (w^T x_i + b) \geq 1 - \xi_i \quad \text{for } i = 1, ..., l \\ &\qquad \xi_i \geq 0 \qquad\qquad \text{for } i = 1, ..., l \end{aligned} \tag{4}$$

In (2), ξ_i are non-negative variables which bring training errors into the scene. The penalty factor C, also called regularization factor, is always positive. In case it is small, the separating hyper-plane is more focused on maximizing the margin (m) while the number of misclassified points is minimized for larger C values. Support vectors which include the points closest to the optimal hyper-plane maintaining maximum margin, satisfying (2) with equality sign, are required to obtain the separating hyper-plane.

The classification problems in practice are usually not linear. To implement SVMs for such cases, so called kernel functions are deployed for mapping training data by the use of nonlinear transform function $\phi(x_i)$:

$$\phi(x_i) = \left(\phi_1(x_i), ..., \phi_m(x_i) \right), \quad \text{where } m > n \tag{5}$$

The equation which could define a kernel function is: $K(x_i, x_j) = \phi(x_i)^T \phi(x_i)$. Having

done such a mapping, the goal is to be able to implement the linear classification of the original input data x in the higher-dimensional space using linear SVM formulations.

Although SVMs are designed to be deployed for the binary classifications, they could be used for multiclass classification purposes too. Generally, there are three approaches to implement a multiclass SVM: one-against-one (OAO), one-against-all (OAA), and one-step methods. The first two approaches are based on combining several binary SVMs; however, in the one-step method the SVM is designed in a way to include all the classes at once during the learning algorithm and solve only one optimization problem [86-88]. The performance comparison between these three methods has shown that the one-step approach gives better accuracy in addition to be faster than the others [58]. Hence, this method is chosen here.

In one-step method, the idea is to create p two-class rules which are separated by p decision functions. For example, the vectors of class k are separated from the other vectors by the kth function $w^T\phi(x) + b$. However, all the decision functions are obtained by solving one problem as follows:

$$\begin{aligned} \min \ & \frac{1}{2}\sum_{k=1}^{p} w_k^T w_k + C\sum_{i=1}^{l}\sum_{k\neq y_i} \xi_i^k \\ & w_{y_i}^T \phi(x_i) + b_{y_i} \geq w_k^T \phi(x_i) + b_m + 2 - \xi_i^k \\ s.t. \quad & \xi_i^k \geq 0 \quad \text{for } i = 1,...,l \ \& \ k \in \{1,...,p\} \setminus y_i \end{aligned} \tag{6}$$

And the decision function is:

$$\text{argmax}_{k=1,...,p}\left(w_k^T \phi(x) + b_m\right)$$

6.3.2. Kernel Function Selection

Various kernel functions have been proposed by researchers such as linear, polynomial, radial basis function (RBF), and sigmoid kernel functions. In this study, RBF kernel $F(x_i,x_j) = \exp(-\gamma||x_i - x_j||^2)$ for $\gamma > 0$ is considered as a reasonable first choice because of several reasons. Deploying RBF kernel provides non-linear mapping of input data sets and is able to deal with the non-linear correlation of the class labels and features, so it overweighs the linear kernel [88]. Besides, a linear kernel is considered as a subset of RBF because for a definite penalty factor, *C'*, it could be represented as the RBF kernel having specific parameters (C, γ) [89]. Sigmoid kernel also performs like RBF for certain parameters [90]. Moreover, there are some parameters for which the sigmoid kernel is not the dot product of two vectors, so it is not valid [86]. Polynomial kernel has more unknown parameters to be determined compared to RBF kernel and this makes the model selection for polynomial kernel more complex. Furthermore, polynomial kernel values might be not properly bounded. Last but not least, numerical difficulties for the RBF kernel are fewer than the others [88].

6.3.3. Parameter Selection

C and γ are two unknown parameters which should be determined when using RBF kernel. Proper parameter search must be conducted on the grid of data to find the best of these values for a given problem. The focus is on finding (C, γ) values for SVM classifier to be able to predict the unknown data, i.e. testing data set, accurately. A common approach is to provide two sets of data which are called training and testing or known and unknown data sets respectively. The SVM performance is better evaluated by prediction accuracy

obtained from classifying the unknown independent data set. This process is called cross-validation in its advanced form.

In this study, C and γ are obtained by conducting a grid-search using cross-validation. To implement n-fold cross-validation, the training data set is divided equally into n subsets of data. Then, to test each subset, the SVM is trained on the remaining ones (n-1 subsets) so each training instance is tested once, and training accuracy represents the number of subsets which were classified correctly. This technique is useful in preventing the over-fitting problem [88].

6.4. Proposed Methodology

6.4.1. Identifying the Vulnerable Relays

To implement the proposed protection scheme, first, the relays which settings coordination might get affected due to unintended DG tripping should be identified according to the network topology. The automatic distance setting coordination check module previously proposed in Section 5 can be utilized to identify the vulnerable relays to the network topology change in terms of DG tripping from the steady state perspective. The power flow data for two cases of with and without DG in the system is given as the input to the setting adequacy check module. The module would identify the relays prone to misoperate according to their current settings and sort them as the critical relays for which the SVM-based detection could be implemented. At the substation level a SVM-based protection scheme is proposed, as discussed in the following Sections, which can be trained to capture the interactions of system's dynamic behavior with distance backup protective zones as a result of DG tripping and enable the candidate relays to

distinguish between a fault and such an event.

6.4.2. Proposed SVM-Based Protection Scheme

In this part of the dissertation a SVM based protection scheme which enables the distance relay to distinguish between a fault and a DG tripping scenario when interfering with the protection coordination of distance backup protective zones is proposed. The detection is based on the DG tripping impact on the system dynamic behavior. As shown in Figure 21, two multiclass SVMs are deployed, one is trained based on local data only (SVM-1) and the other one is provided with system wide measurement data as well

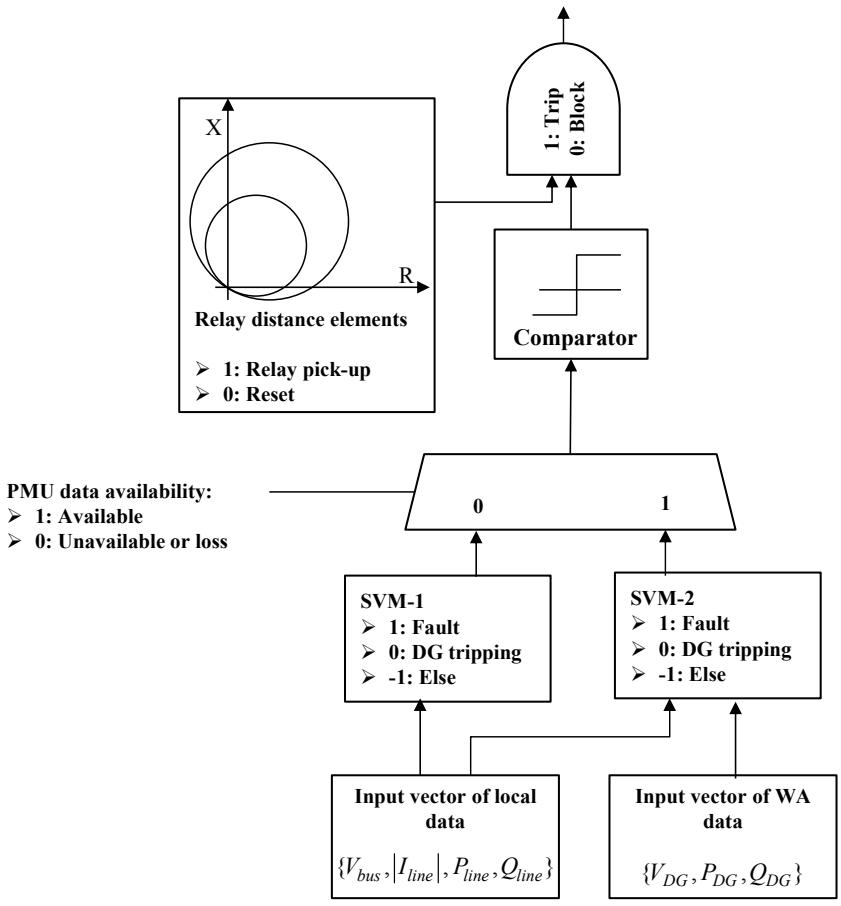

Figure 21. Block diagram of the proposed scheme

(SVM-2). Based on whether the PMU data is being received at the relay location or not, the method could switch between the employed SVMs outputs through the multiplexer shown in Figure 21. This is for maintaining the scheme's robustness under probable PMU data unavailability or loss; however, the accuracy may decrease to some extent when using local data only as will be discussed later in the case study section. SVM-1 and SVM-2 are trained to classify fault, DG tripping, and other cases as "1", "0", and "-1" respectively. The outputs of these SVMs are filtered by a comparator as class label -1 is not of interest. The logical AND of the backup protective zones pickup signal and the output of the comparator, as shown in Figure 21, determines the trip/block signal value, i.e. 1 or 0.

A proper modeling of the DG units is important to get a fair observation of their impact on the dynamic behavior of the network following a disturbance. In this research, the focus is on PVs in the distribution level (residential PVs) which are modeled as constant current loads corresponding to the negative power injections, which is used in other studies of this type [28, 35, 91]. The equivalent of DG units aggregated based on their generation type from the transmission perspective could be represented as shown in Figure 22 [28, 35]. For studies of this type, the downstream distribution network,

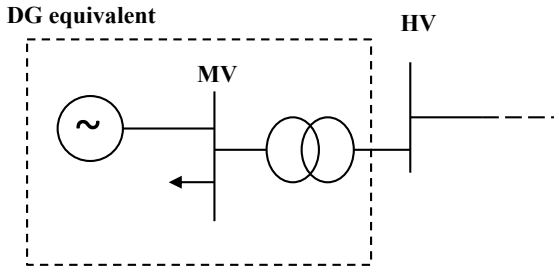

Figure 22. DG plants equivalent from the transmission side

regardless of its connections, is modelled as the aggregated load and distributed generation imposed on the upstream network from the transmission point of view [28, 35]. This accepted type of modeling is especially appropriate when the distribution grid is connected to a well interconnected and stable upstream network, as is the case in this study. The cluster of PVs is modeled as an equivalent power output equal to the sum of individual outputs of each one of the units [28, 35]. It is worth to note that DGs are usually operated in constant power/power factor control mode [29]. From the transmission point of view, different types of DG would not be experienced significantly different from each other. Under specific cases of DG operation, if the majority of the DGs are facilitated with voltage regulation or speed controls based on their type, they should be modeled correspondingly [28]. We have focused on PVs because of their modeling simplicity. They are considered as the most promising type of DGs growing fast in the distribution level because of their economic and environmental incentives [35].

Local measurements and calculations based on them at the relay point are the required elements of almost all of the protection schemes. Features selected from the local measurements as inputs for the SVM-1 and SVM-2 are: V_{bus}, $|I_{line}|$, P_{line}, and Q_{line} representing the bus voltage phasor, line current phasor magnitude, line active and reactive power flow respectively. Thanks to the PMU technology, system wide measurements from various points of the system could be provided in today's power system operation. When employing system wide measurements technology, implementation cost must be considered for the method to be economically justifiable. In other words, the more PMUs are deployed; the significantly higher implementation cost would be experienced although

a better system behavior observation may be obtained. It is assumed that phasor measurements from PCC and target relay bus in regard to the reference bus are available and by PCC, as shown in Figure 1, only the distribution to upstream connection bus is meant rather than all of the DG units' interconnections individually. Therefore, implementing the proposed method would be economically practical. Net active (P_{DG}) and reactive (Q_{DG}) power injections from the PCC into the transmission grid calculated from the PCC's PMU measurements are two good features to be utilized to improve the SVM-2 pattern recognition and classification accuracy. The other proper feature is the voltage phasor at the PCC on the grid side (V_{DG}). Deploying these measurements and calculations is specifically beneficial to improve the SVM's performance accuracy when classifying under more complicated scenarios such as detecting a second fault when the system is already under the stress of a post fault and subsequent DG tripping events. As it will be shown in the case study section, the proposed scheme is able to detect such cases and unblock the trip signal, so the protection security and dependability is well maintained.

Depending on the application of the PMU, the role of communication requirements and latencies could get highlighted. The delay related to PMU deployment is caused from three main processes: phasor creation, transmission of data through the available communication link, and merging of data streams in phasor data concentrators (PDCs) [92]. The PMUs use fast mathematical algorithms, such as discrete furrier transform (DFT) and calculate the voltage and current phasors from RMS measurements obtained by voltage and current instrument transformers [92]. Then the phasor measurements are transmitted according to IEEE C37.118 [93] data format to PDCs via available

communication link and the delay depends on the link's data transfer capability, the size of the PMU data output, as well as physical distance between PMU and PDC. The PDC delay, at the target substation in this study, corresponds to implementing time tag on the data and preparing a system-wide measurement [94]. There are various communication options available for wide area measurement system (WAMS) including telephone lines, fiber-optic cables, satellites, power lines, and microwave links [92]. Studies show that the average combined delay caused by the above-mentioned reasons over even long transmitting distances (in the order of 1000 miles) when using a communication media with a band-width of 56Kbps (data rate in telephone lines) is around 5-7 cycles of a 60 Hz system [94]. Therefore, deploying wide area measurements in the proposed method is a proper fit with regards to the method's application for the purpose of improving distance relay back-up protection which, as mentioned before, operates with a time delay (20 and 60 cycles for zones 2 and 3 respectively). Deploying advanced communication media such as fiber-optic cable by utilities provides a data transfer speed up to 2Mbps and significantly reduces the delay by removing the delay corresponding to the PMU data size [92].

The SVMs training scenarios includes different DG tripped capacities following 3-phase faults on the transmission side at various points in the vicinity of the DG placement in order to have realistic scenarios of the severe disturbance impact propagation from transmission to distribution level. The possible DG tripping instant following the disturbance varies in a range assumed according to the standards for anti-islanding protection schemes. Having prepared the training data set the SVMs go through the learning process and their performances are verified on the testing data set as will be

discussed in the following Section.

Employing SVM technique to approach the problem under consideration from the distribution side, when using local data only, may not be a proper fit. To maintain its operation accuracy under the probable upstream disturbances might be challenging. After all, the primary issue was raised when deviations propagating from transmission to the distribution side are close to and almost not differentiable from those caused by islanding situation which is a probable thread to any anti-islanding protection scheme. Under such circumstances, the accuracy of SVM may be affected if only relying on local measurements because training the SVM to differentiate between such cases actually means training it for instances with similar features yet different labels which lowers the classification accuracy. The unintended DG tripping risk still remains unless remote measurements are provided for each DG unit's interconnection relay which is the same as the costly method of transfer trip.

6.5. Case Study

The simulations have been conducted on the New-England 39-bus test system [95], Figure 23. Having conducted a sensitivity analysis on the test system using the setting coordination check module proposed in Section 5, the buses for clustered DG location with higher impact on the network distance relay settings and their corresponding list of critical relays (target relays) are identified. It was concluded that clustered PVs on bus 27, as shown in Figure 20, is one of the locations with highest impact on distance relay settings for unintended PV tripping cases and the corresponding list of critical relays to this location is brought in Table 5.

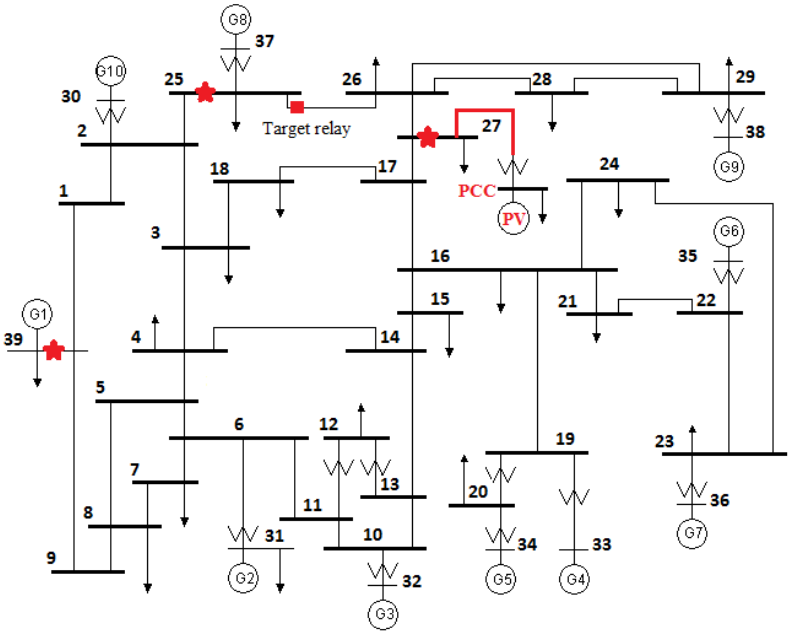

Figure 23. One-line diagram of New-England 39 bus system with DG penetration

Maximum PV penetration in the system is assumed to be a considerable amount of 500 MW all of which has been tripped to sort the vulnerable relays in the system as the worst-case scenario. The penetration level could be defined in various ways based on the system's total generation, system's peak load, or amount of energy served [35]. For example, considering the system's total generation, the penetration level is obtained from the following equation:

$$\text{DG Penetration (\%)} = \frac{\text{Total DG generation (MW)}}{\text{Total generation (MW)}} \qquad (7)$$

That is around %10 in this study.

For this study, the amount of the DG tripped capacity, the instant of the tripping

Table 5. Vulnerable relays to DG tripping

Rank	Critical Relay
1	$R_{25\text{-}26}$
2	$R_{29\text{-}26}$
3	$R_{16\text{-}17}$

following the disturbance on transmission side, current distance relay settings, etc., which play the key role in the protection coordination interference, are more important than the total level of penetration.

The proposed method is implemented for the most critical relay ($R_{25\text{-}26}$), which is considered as the target relay. As mentioned before, the PMUs are assumed to be located on the reference bus (bus 39), the target relay bus (bus 25) and DG PCC as shown by stars in Figure 20. The SVMs are trained for the unintended DG tripping scenarios seen by the target relay. Simulations have been performed by PSS/E software on a PC with an Intel Xeon W3530 C 2.8 GHz CPU. LIBSVM is used to train and test the SVMs [87, 96].

6.5.1. Creating the Training and Testing Data Sets

The SVM training data set consists of different cases (84 cases in total) including: 3 DG tripped capacities (100 MW, 250 MW, and 500 MW), faults on transmission system at different distances in the vicinity of the DG placement, which also includes some points along the lines in the third zone of the target relay, and multiple DG tripping instants following the disturbance. According to the IEEE standard, the anti-islanding schemes should be able to detect all possible islanding conditions and trip DGs within 0.16 to 2

seconds depending on the level of voltage and frequency variations [84]. The reporting rate of the PMUs is considered 60 phasors per second in a 60 Hz system according to the standard [93]. It should be noted that this is different from the PMU sampling rate on the input signal. The sampling rate might be up to 512 samples per cycle [93]; however, one phasor per cycle is computed and reported by the PMU. Each instance of training includes 2 cycles of data. As mentioned before, the local measurements include V_{bus}, $|I_{line}|$, P_{line}, and Q_{line} at the target relay location. Deploying the PMU technology, V_{DG}, P_{DG}, and Q_{DG} at the DG PCC are also available. Note that the voltage phasors measurements include both magnitude and angle. Therefore, considering 1 phasor per cycle reporting rate and length of each instance (2 cycles), the input vector for each instance of training consists of 10 (5×2) features from local measurements and 8 (4×2) from system wide measurements. Hence, the input vectors for SVM-1 and SVM-2 consist of 10 and 18 features respectively. Considering all the simulated training cases, i.e. 84 cases of one-and-half seconds system operation time, the training set consists of 3780 instances. The same procedure is taken to create the testing data set. The conditions including DG tripped capacity, fault location and instant of DG tripping, are chosen intentionally different from the training set to assess the performance of the SVMs for unseen scenarios. In total, there are 1692 instances in the testing data set. Different types of DGs and their modeling might cause a change in the measurement values of the selected features and the SVMs should be trained based on the updated values correspondingly.

6.5.2. SVM Parameters Selection, Training, and Testing

The next step is to select SVMs parameters efficiently. It can get time consuming

to choose the best parameters in case proper selection cannot be drawn from the available knowledge on the problem and a systematic approach is not taken. An interactive grid search approach has been taken here to evaluate the training generalized accuracy. A five-fold cross validation is implemented by dividing the training data set into 5 subsets of data. It is found that an effective approach to obtain proper values for the pairs of (C, γ) is to try growing their sequence of values exponentially. In order to avoid a complete grid search which is time consuming, first, a bigger incremental step is chosen for the sequence of values, e.g. $C = 2^{-5}, 2^{-3},\ldots, 2^{15}$ and $\gamma = 2^{-15}, 2^{-13},\ldots, 2^{3}$, which is called a loos grid search to find a proper region on the grid of data. When the proper parameter values are found, another search with smaller incremental step is conducted around the values, which is called fine grid search, to find any better value for the parameters. The graphical presentation of generalization contours for the SVMs after a five-fold cross-validation is shown in Figure 24 in which (a)-(b) and (c)-(d) corresponds to SVM-1 and SVM-2 for loos and fine searches on training grid of data respectively. Although the accuracies for the cases seen in Figure 24 are not significantly different, it should be noted that this is training accuracy which does not replicate the SVM performance fairly as the class labels are known. To verify the SVM actual performance, it should be evaluated on a data set with unknown labels to observe the testing accuracy. As it could be seen from Figure 24, proper values for the pairs of (C, γ) for SVM-1 and SVM-2 are determined to be (8192,4) and (1024,0.5) respectively. The parameter selection process has been accomplished in less than 10 minutes.

Having found the proper parameters values, the SVM-1 and SVM-2 are trained and

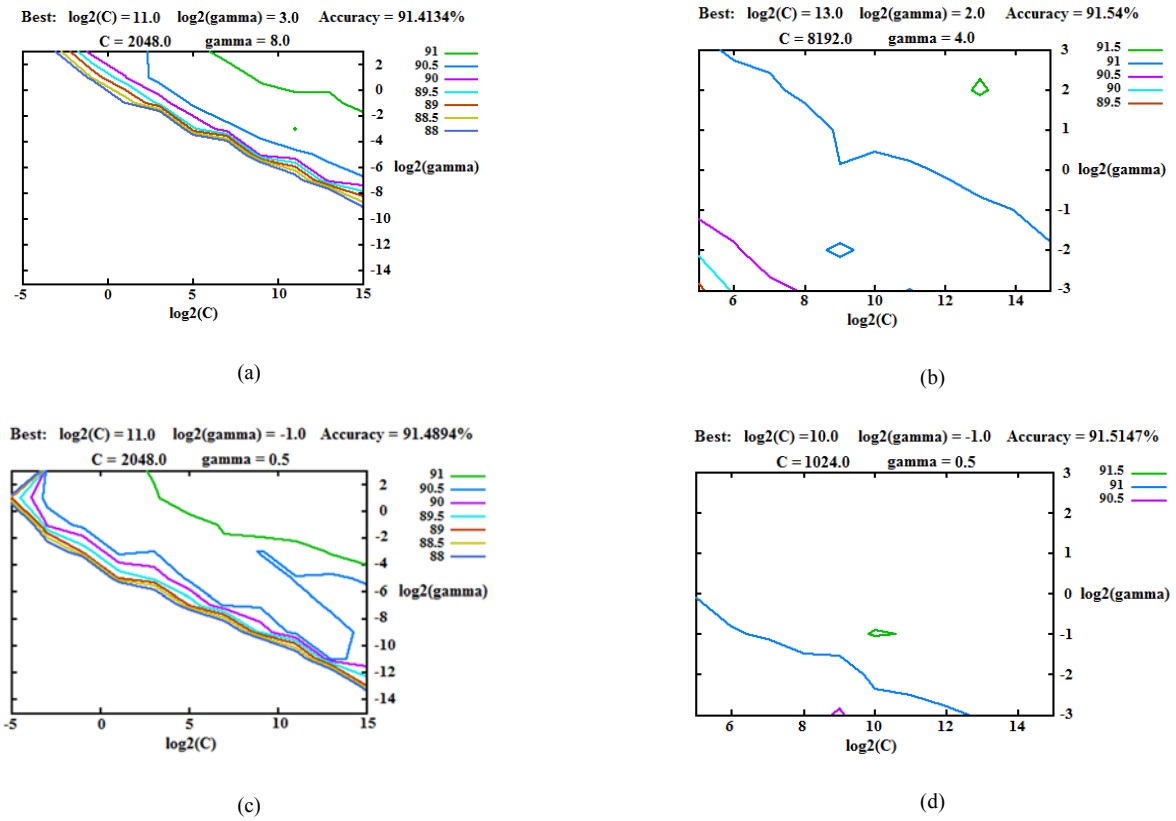

Figure 24. Interactive grid search using cross-validation for selecting SVMs parameter values; (a)-(b) loos and fine searches on training data-set for SVM-1; (c)-(d) loos and fine search on training data-set for SVM-2

tested for their corresponding sets of data. Table 6 shows the SVMs specifications and classification accuracy obtained in both cases of using local measurements only (SVM-1) and including system wide measurements as well (SVM-2). As it could be seen, the classification accuracy has been increased to a very desirable level when employing system wide measurements; however, an acceptable accuracy is still achieved while using local measurements only. This assures the robustness of the method against PMU data unavailability. In addition, the insignificant training and testing time for SVMs as shown

Table 6. SVMs specifications

SVM No.	SVM-1	SVM-2
C	8192	1024
γ	4	0.5
No. of Iterations	2112058	98096
No. of SVs	772	753
Testing Accuracy (%)	93.8	97.6
Training Time (s)	39.67	8.76
Testing Time (s)	0.147	0.19

in Table 6, infers the easy implementation and practicality of the proposed method.

Figure 25 compares the outputs of SVM-1 and SVM-2 for a testing DG tripping scenario. The testing scenario is that a 3-phase fault happens on x = 0.3 of the line 26-29

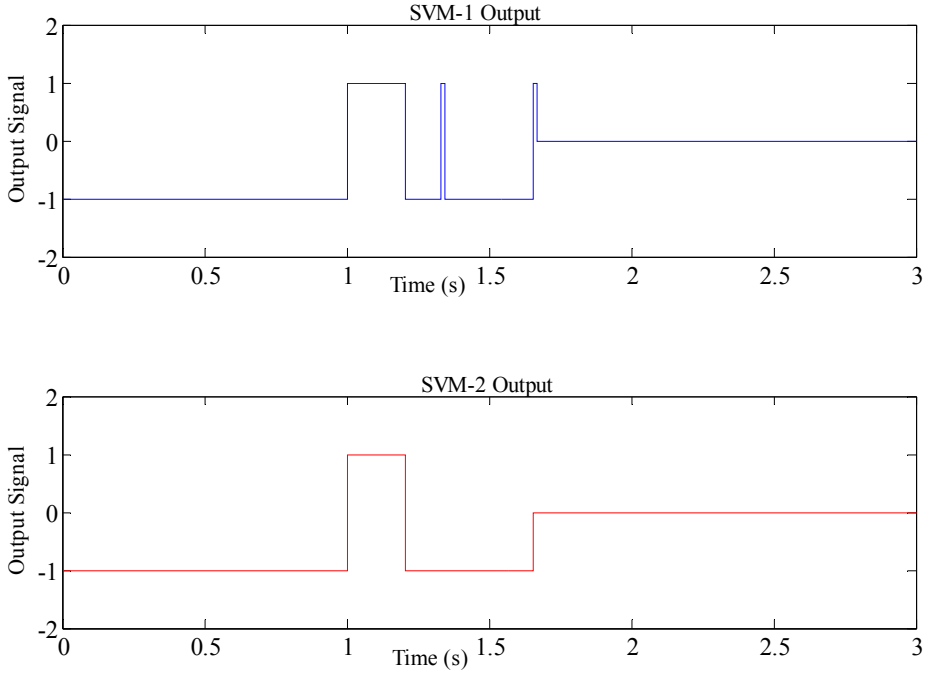

Figure 25. SVMs output comparison under the DG tripping scenario

at t = 1s and cleared at t = 1.2s by tripping this line out. As a consequence of miss-detection of PV interconnection relays on the distribution side, at t = 1.65s, 250 MW PV is tripped unintentionally. The signal values of "1", "0", and "-1" represent the fault, DG tripping, and other status respectively. As it could be seen both SVMs have classified the instances well. The temporary spikes seen in SVM-1 output (at t = 1.35s or t = 1.65s) are as a result of miss-classification; however, they do not affect the relay operation since they are not persistent.

As mentioned before, employing the PMU measurements from PCC improves the accuracy of the SVM especially under more complicated scenarios of classification. To verify this, the above-mentioned scenario has been complicated by the occurrence of a second fault on x = 0.4 of the line 26-28 at t = 2.5s when the system is already experiencing the stress caused by previous fault and subsequent DG tripping. The SVMs' performance under this scenario is illustrated in Figure 26. As it could be seen, SVM-2 has classified the instances with a better accuracy compared to SVM-1, i.e. lower number of misclassifications, especially during the second fault detection. Figure 27 compares the proposed method output, i.e. trip/block signal in Figure 21, with the legacy distance relay pickup on the above-mentioned testing scenario. As it could be seen, following DG tripping, the distance element of the target relay backup zone (zone 3) has picked up from t = 1.8s to the end while the proposed method blocks the relay operation during DG tripping interference and unblocks it at t = 2.5s when the second fault happens.

Table 7 summarizes and compares the performance of the SVMs in classifying the instances. As it could be seen from Table 7, the numbers of correctly detected cases of

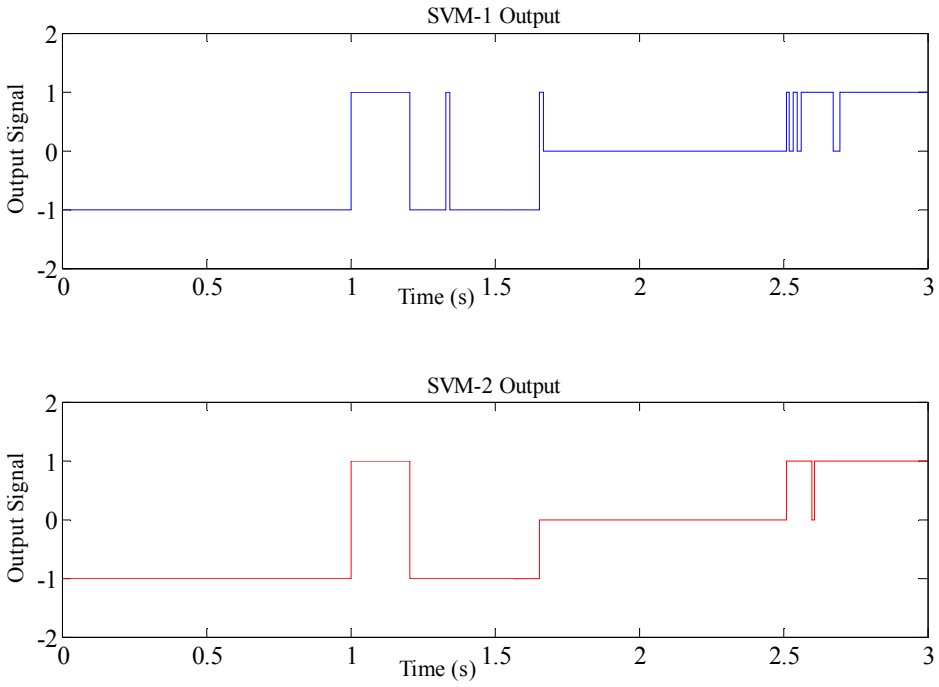

Figure 26. SVMs output comparison for a fault during the DG tripping scenario

faults, DG tripping, and others are higher when deploying SVM-2. In other words, the protection dependability and security has been better maintained when using system wide measurements. The accuracy in Table 7 is the ratio of the number of correctly detected instances of a type (e.g. fault) to the actual number of instances of that type. As mentioned before, the fault instances include complicated fault scenarios, i.e. a second fault happening on transmission side following DG tripping event, to test the dependability of the proposed method in addition to the security. To have an estimate on the proposed method's dependability for normal fault situations on the transmission side, i.e., faults which are not following the DG tripping event, a total 117 of such fault cases were run and SVM-1 and SVM-2 performed detection with 99.1% and 100% accuracy respectively.

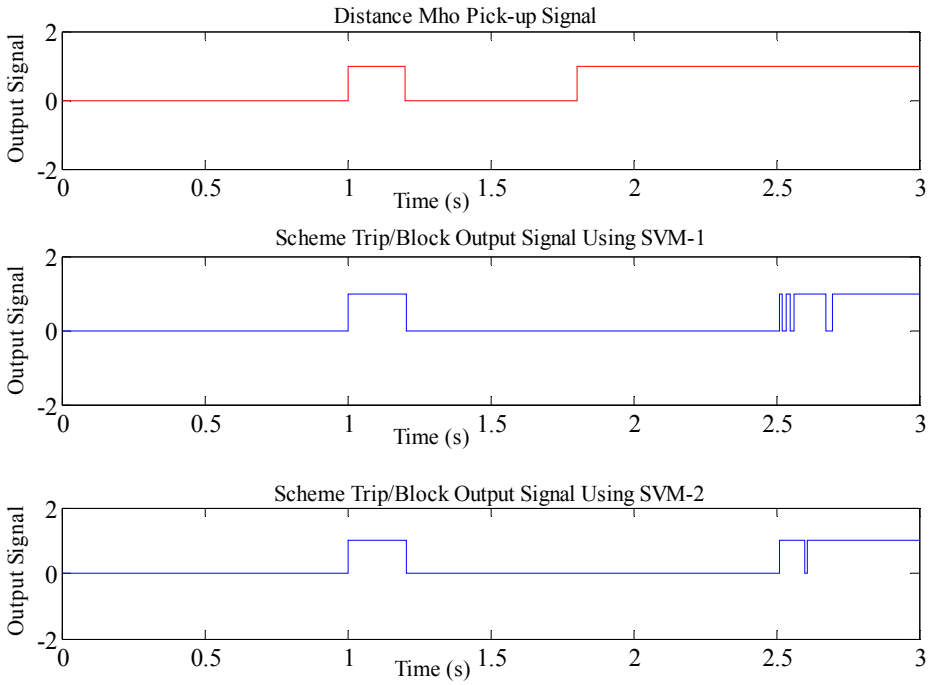

Figure 27. Comparison of the proposed method output with the conventional distance pickup

6.6. Conclusions

The main contributions of this part of the research are as follows:

- A SVM-based protection scheme which prevents maloperation of distance relays in unintended DG tripping scenarios is proposed.
- WA measurements have been used in addition to local measurements to increase the SVM's classification accuracy and that of the protection scheme consequently. The proposed scheme is robust against PMU data loss or unavailability.
- Unlike conventional blocking schemes, the proposed protection scheme not only blocks the relay following the interference of a DG tripping scenario

Table 7. SVMs performance comparison

Type of Instance		Fault	DG Tripping	Others
Actual No. of Instances		263	897	532
No. of Detected Instances	SVM-1	284	913	495
	SVM-2	270	891	531
No. of Correctly Detected Instances	SVM-1	240	860	488
	SVM-2	251	874	527
No. of Incorrectly Detected Instances	SVM-1	44	53	7
	SVM-2	19	17	4
Accuracy (%)	SVM-1	91.3	95.9	91.7
	SVM-2	95.4	97.4	99.1

with distance coordination but also detects a fault if it happens during the blocking period and unblocks the relay to operate properly.

- Since the proposed scheme is easily and quickly trainable, it is applicable to various possible practical system operation scenarios and gives significant selectivity.

In summary, deploying the WA measurements infrastructure not only improves the scheme accuracy but also makes it independent of the aggregated DG location in the system. The proposed scheme could be implemented in combination with other protection schemes such as power swing blocking to help maintaining power system protection dependability and security.

7. CORRECTIVE PROTECTION: REAL-TIME RELAY MISOPERATION DETECTION TOOL

7.1. Introduction

Distance relays may misoperate by seeing the fault in a protective zone by mistake when the fault is actually in another zone or out of zones of the relay. This is a no-fault condition which is seen as a fault within a protective zone of the relay, e.g. power swings; etc. When a relay operates, an on-line fault analysis can identify whether it has operated correctly. If this analysis is performed with a sufficiently high speed, it can be employed in the last step of an auto-reclosing action allowing enough time to produce results to correct a misoperation of the relay. Assume a re-closer has detected a fault and operated once, i.e. first trip, and it is waiting before it implements the second closing action. If the fault has happened outside the protective zone of the relay and it has operated incorrectly, the situation may repeat and cause a lock out (complete trip) after the reclosing action. With the use of the real-time fault analysis and relay misoperation detection approach, such tripping and locking out by the re-closer can be supervised and avoided. The interval between re-closers' closing actions can also be set properly to accommodate and let for utilizing the fast misoperation detection module output for supervisory control.

The fault analysis approach based on fast synchronized sampling with high accuracy as well as event tree methods proposed in [41], [69-70] is utilized here to implement a relay misoperation detection tool at the substation level. Should a re-closer operate, the tool is activated to verify the operation correctness of the relay and in case of detecting any misoperation, the system can be saved from experiencing an unnecessary line outage. Very high speed of fault analysis is aimed to be achieved by the proposed

method such that it can be deployed to impact and improve the re-closing applications.

7.2. Methodology

Figure 28 depicts a typical transmission line setup with the event-triggered measurements from both ends. As it can be seen, the line can be monitored by different substation Intelligent Electronic Devices (IEDs) at both ends (details are only shown in substation 1). When a fault (or disturbance seen as a fault by the protective device) occurs, several IEDs can be triggered and they will capture event measurements. The assumption is that the data samples are synchronized and time-stamped using the Global Positioning System (GPS), and a high-speed communication link between substations and control center is available. The relay misoperation detection tool implementation is illustrated in

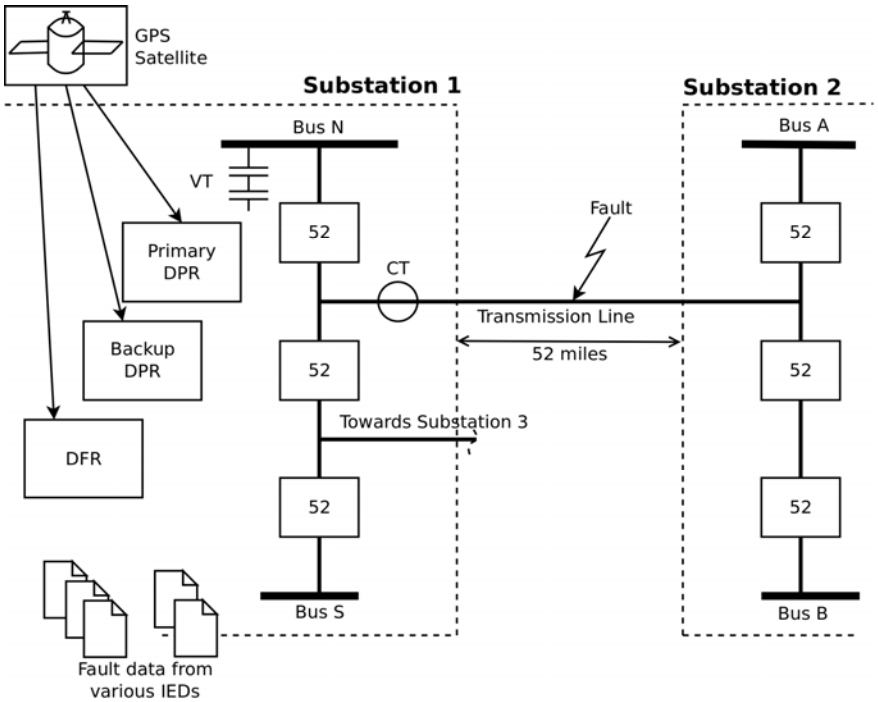

Figure 28. Typical transmission line setup with measurements from both ends

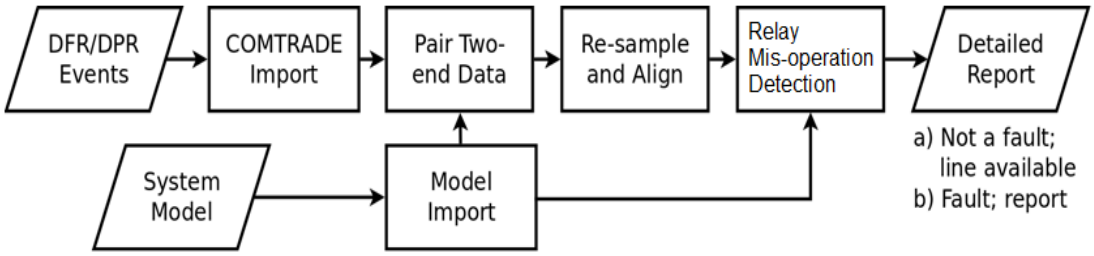

Figure 29. Automated analysis of time-synchronized event data (Relay misoperation detection tool)

Figure 29. Following is the description of each step.

Step 1. DFR/DPR Events Import: The required IED device data consists of voltage and current samples captured by DFR or DPR. The fault data and system model data are necessary inputs for the tool to run and operate correctly and accurately. The involved DFR and DPR devices varied by vendor, types, and vintage. All data files from different vendors have been converted in unified COMTRADE file format (IEEE C37.111-1999).

Step 2. System Model Import: The system model topology is obtained from the PSS/E (*.raw) file and used for pairing the event files coming from two ends of the same transmission line.

Step 3. Pairing the Two-end Data: There can be multiple IED files created during a disturbance at different substations. Utilizing the network topology from the system model, the IED files from the neighboring nodes are paired to extract the two-end measurement data corresponding to the transmission line between the buses.

Step 4. Re-sample and Align: After the two-end data are paired, they are processed in order to extract data samples for instantaneous voltage and current signals measured at both ends of the line. The extracted data samples are re-sampled and aligned (when the

triggering time was not the same) in order to obtain the same sampling rate at both ends as well as synchronized samples.

Step 5. Relay mis-operation detection: The relay mis-operation detection tool core algorithm has been introduced in [41], [69-70] as mentioned before. Here, an overview of relay mis-operation detection core algorithm implemented as a part of the proposed tool is provided. In Figure 30, $V_1(t)$ and $I_1(t)$ represents voltage and current measured at one end (Bus 1) of the line at instance t. Similarly, $V_2(t)$ and $I_2(t)$ represent voltage and current measured at the other end (Bus 2) of the line respectively. Instantaneous powers calculated at both ends are: $P_1(t) = V_1(t) \times I_1(t)$, and $P_2(t) = V_2(t) \times I_2(t)$.

During the normal operation, $P_1(t)$ and $P_2(t)$ will be in phase opposition to each other for the current directions assumed. However, for the faulty phases, when the fault is initiated, they will be in-phase with each other. For un-faulted phases the phase opposition will be maintained even after the fault inception. If a load level change or a fault in neighboring line occurs, the calculated instantaneous powers will remain in opposite direction. Therefore, the method can discriminate load level changes or external faults from internal ones. To represent this feature mathematically, signum function is employed

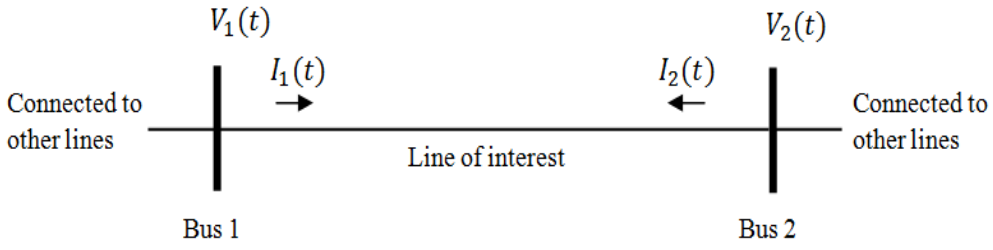

Figure 30. Transmission line with two-end measurements

and defined as:

$$\mathrm{sgn}(x) = \begin{cases} -1, & x < 0 \\ 0, & x = 0 \\ 1, & x > 0 \end{cases} \qquad (1)$$

$\mathrm{sgn}(P_1(t))$ and $\mathrm{sgn}(P_2(t))$ are calculated and their difference is obtained for each phase as:

$$P\mathrm{sgn}(t) = \mathrm{sgn}(P_1(t)) - \mathrm{sgn}(P_2(t)) \qquad (2)$$

Theoretically, before a fault has been initiated, this difference $P\mathrm{sgn}(t)$ should be +/-2 and after fault occurrence $P\mathrm{sgn}(t)$ should be 0 on all faulty phases. The change of difference of sgn(t) is utilized as a signal to detect fault instant from (2). However, due to transients and noise in the measurements, some outliers exist. To avoid incorrect decisions caused by outliners, a moving window of 5 ms is used to check whether at least 80% of $P\mathrm{sgn}(t)$ are zero, which indicates a fault.

Step 6. Results: The results of relay mis-operation detection tool are provided in real-time to be utilized in supervising the reclosing process. As shown in Figure 29, the outcome of the analysis may be: a) no fault, which means that the tripped line may be available to switch back in; b) fault detected and operation of relay has been confirmed, which means no need for further reclosing attempts.

7.3. Case Study

The relay mis-operation detection tool has been tested against various simulated and field data test cases. The following two examples demonstrate how the tool behaves in the case of a fault as well as relay mis-operation. In both cases, the sampled data are

taken from actual IED device in field.

As shown in Figure 31 (a-c), the instantaneous powers from two ends at phase B

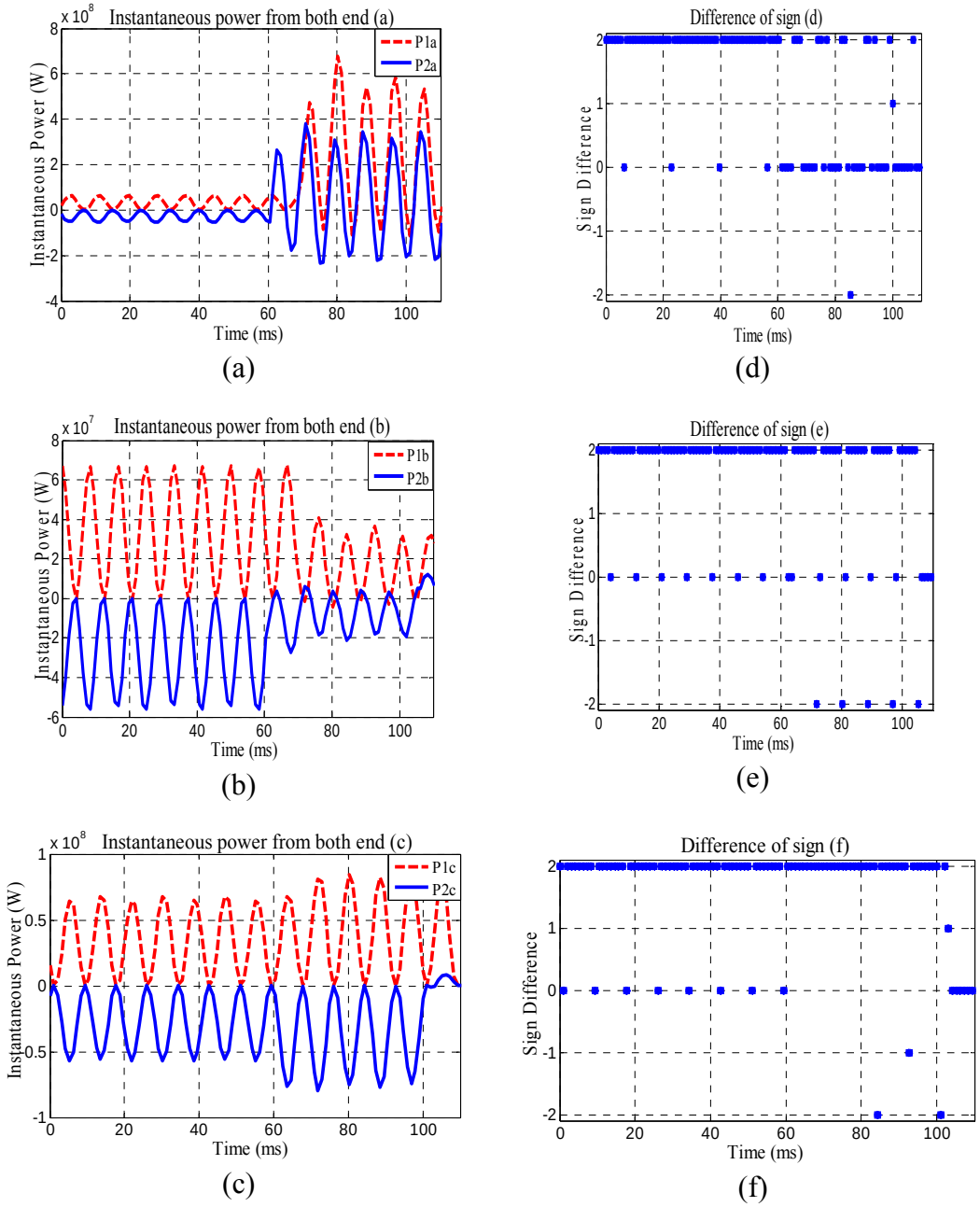

Figure 31. Single phase to ground fault detection and classification

and C are in the opposite direction before and after disturbance. While in phase A, the direction has been changed after fault initiation time. As a result, the output of the relay mis-operation detection tool results in the detection of "phase A to ground fault". Figure 31 (d-f) depicts plot of $P\text{sgn}(t)$ with respect to the time for three phases. It can be seen that in phases B and C less than 80% of the total samples are zero. However, more than 80% of the total samples of phase A is zero.

Figure 32 shows the same type of output plots for a relay mis-operation test case. Figure 32 (a-c) depicts instantaneous power $P_1(t)$ and $P_2(t)$ calculated based on data captured by DFR units at the two ends of transmission line with respect to time. In this case, the information received by utility shows that the fault occurred on a neighboring line. The line has been falsely tripped as a result of the relay misoperation due to a single-phase fault on an adjacent line according to the later investigation of the case.

From Figure 32 (a-c) one can observe that the opposite direction of instantaneous powers from two ends stay the same before and after disturbance. As a result, the output of the tool indicates "no fault" condition. Figure 32 (d-f) shows plot of $P\text{sgn}(t)$ with respect to time for three phases. It can be seen that less than 80% of the total samples are zero which means no fault has been detected in any of three phases. This detection happens in less than 5ms which is very desirable to be able to be accommodated in the reclosing applications. It should be noted that the reclosing attempts happen with intervals from 20ms (first reclosing attempt after the initial trip) up to a few seconds after the initial trip depending on the number of reclosing attempts and interval settings between them [97-98].

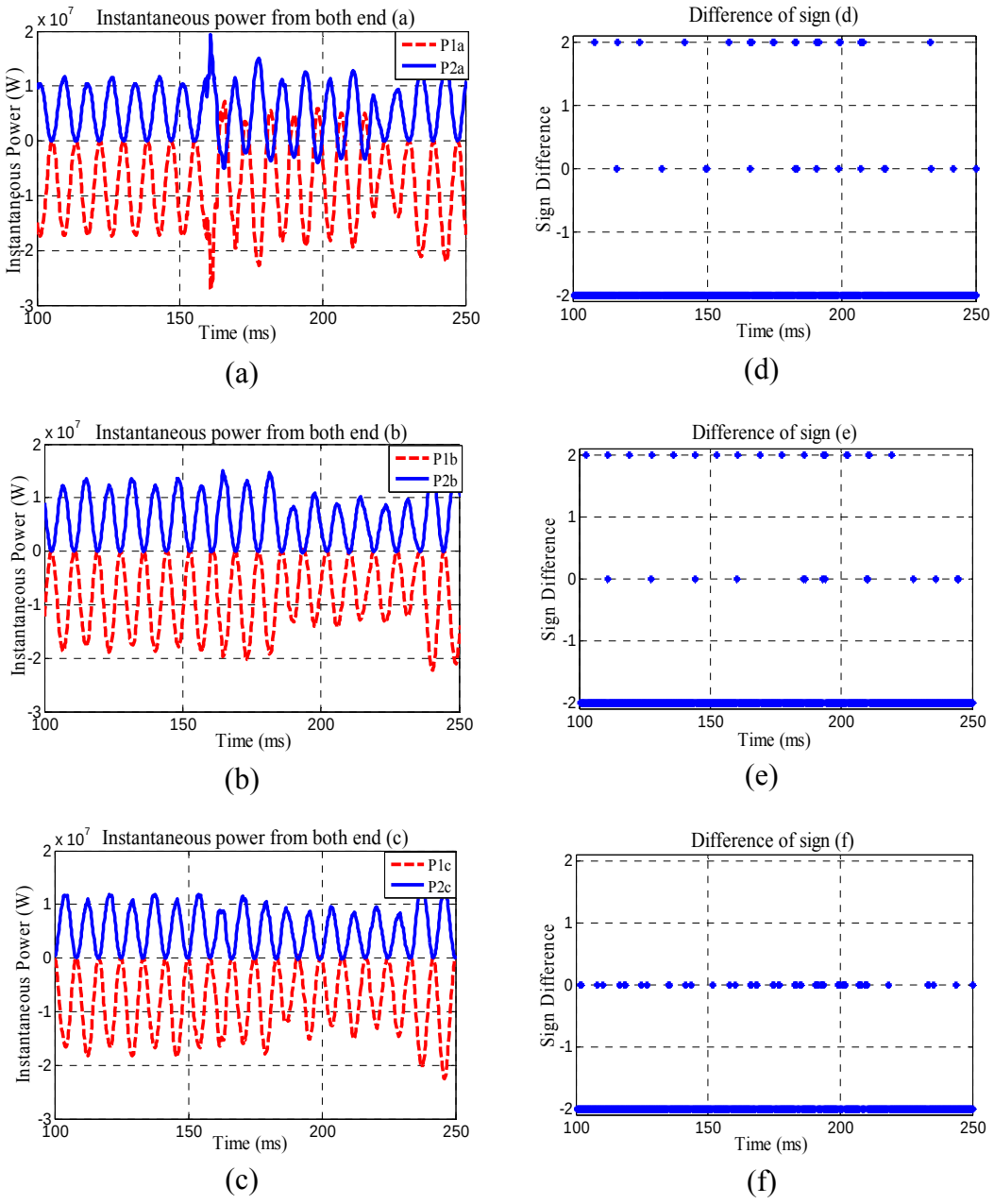

Figure 32. Relay Mis-operation Detection

7.4. Conclusions

The main contributions of this part of the research are as follows:

- A simple and effective fault analysis approach using synchronized samples from both ends of the transmission line is proposed which can be utilized as a relay misoperation detection tool
- The method is very fast and accurate, so it can be used in a real-time manner to supervise the reclosing process and avoid/allow extra reclosing attempts depending on the fault analysis results
- The proposed method can be utilized in the corrective layer of the fundamental HCP-based supervisory scheme.
- The method is tested for several IEEE and real-life test cases and illustrates excellent performance accuracy

8. CONCLUSIONS

8.1. Research Contributions

The concluding remarks of this dissertation are as follows:

- Investigating the role of power system protection reliability in improving the power system resilience.
- Introducing the system complexities which aim at improving power system resilience as an ultimate goal while can be considered as main contradictory changes from the legacy distance protection scheme.
- Proposing a fundamental HCP-based protection scheme to supervise legacy distance protection function which enables maintaining a dynamic balance between protection dependability and security.
- Proposing an automated distance setting adequacy check module as a solution for the predictive layer of HCP-based supervisory scheme which employs advanced computational technique to implement real-time setting calculation on a real-life network for an evolving network topology.
- Proposing the novel concept of DoI which saves significant computational burden by narrowing down the setting calculations on the affected part of the network rather than the whole of the network.
- Proposing SVM-based protection scheme as a solution for the adaptive layer of the HCP-based supervisory scheme which employs local/system wide measurements and enables the distance relays to maintain the protection reliability under operating concerns as a result of high

penetration of DGs into the system.

- Utilizing a previously proposed real-time fault analysis approach as a relay misoperation detection tool and a solution for the corrective layer of the HCP-based supervisory scheme which can improve the legacy reclosing actions by allowing/avoiding extra reclosing attempts depending on the fault analysis results.
- Testing each of the predictive, adaptive, and corrective solutions on IEEE and real-life test systems demonstrating their performance effectiveness in comparison with the state of the art.

8.2. Suggestions for Future Research

The future works for the research performed in this dissertation could be generally categorized into improving solutions proposed at each layer of the fundamental HCP-based approach or introducing other applications of them:

- The network fundamental (base) topology can be investigated towards achieving an optimized network topology from the system's performance perspective. The impact of the base topology on the system's performance from different viewpoints of protection, stability, reliability, etc. can be of great importance as a potential fundamental approach in improving the power system resilience.
- The potential of improving the computation speed of the proposed setting calculation module by implementing advanced computational and software

module development techniques can be investigated for better results when it comes to real-time applications.

- complementary applications of SVM along with the proposed application in this dissertation can be investigated for achieving a comprehensive adaptive protection scheme to be employed at the adaptive layer of the HCP-based supervisory approach.
- Other applications of real-time fault analysis approaches such as deploying it for improving outage management and restoration can be investigated.

REFERENCES

[1] M. Panteli, and P. Mancarella, "Modeling and Evaluating the Resilience of Critical Electrical Power Infrastructure to Extreme Weather Events," in IEEE Systems Journal, no.99, pp.1-10

[2] M. Panteli and P. Mancarella, "The Grid: Stronger, Bigger, Smarter; Presenting a Conceptual Framework of Power System Resilience," in IEEE Power and Energy Magazine, vol. 13, no. 3, pp. 58-66, May-June 2015.

[3] IEEE PES CAMS Task Force on Understanding, Prediction, Mitigation and Restoration of Cascading Failures, "Initial review of methods for cascading failure analysis in electric power transmission systems," IEEE Power and Energy Society General Meeting, Pittsburgh, PA, USA, July 2008.

[4] A. G. Phadke and J. S. Thorp, "Expose hidden failures to prevent cascading outages," IEEE Computer Applications in Power, vol. 9, no. 3, pp. 20–23, July 1996.

[5] U.S.-Canada Power System Outage Task Force, "Final Report on the August 14, 2003 Blackout in the United States and Canada: Causes and Recommendations," Tech. Rep., Apr. 2004, [Online] Available: http://www.nerc.com.

[6] NERC System Protection and Control Task Force, "Protection System Reliability, Redundancy of Protection System Elements," Tech. Rep., Nov. 2008, [Online] Available: http://www.nerc.com/docs/pc/spctf/Redundancy_Tech_Ref_1-14-09.pdf

[7] M. Chaudry, et al., Building a Resilient UK Energy System. London, U.K.: UK Energy Research Center (UKERC), Apr. 14, 2011.

[8] T. J. Overbye, et al., Engineering Resilient Cyber Physical Systems. Tempe, AZ, USA: PSERC, May 2012, ser. PSERC Publication 12-16.

[9] A Framework for Establishing Critical Infrastructure Resilience Goals, NIAC, Washington, DC, USA, Oct. 2010.

[10] Cabinet Office, "Keeping the country running: Natural hazards and infrastructure," London, U.K., Oct. 2011.

[11] M. Keogh and C. Cody, Resilience in Regulated Utilities. Washington, DC, USA: The National Association of Regulatory Utility Commissioners (NAURC), Nov. 2013.

[12] National Academies of Sciences, Engineering, and Medicine. 2017. Enhancing the Resilience of the Nation's Electricity System. Washington, DC: The National Academies Press. https://doi.org/10.17226/24836.

[13] IEEE Guide for Electric Power Distribution Reliability Indices - Redline," in IEEE Std 1366-2012 (Revision of IEEE Std 1366-2003) - Redline, vol., no., pp.1-92, May 31 2012

[14] V. V. Vadlamudi, O. Gjerde and G. Kjolle, "Impact of protection system reliability on power system reliability: A new minimal cutset approach," 2014 International Conference on Probabilistic Methods Applied to Power Systems (PMAPS), Durham, 2014, pp. 1-6.

[15] E. A. Udren et al., "Proposed statistical performance measures for microprocessor-based transmission-line protective relays. Part I. Explanation of the statistics," in IEEE Transactions on Power Delivery, vol. 12, no. 1, pp. 134-143, Jan 1997.

[16] E. A. Udren et al., "Proposed Statistical Performance Measures for Microprocessor-Based Transmission-Line Protective Relays, Part 2: Collection and Uses of Data," in IEEE Power Engineering Review, vol. 17, no. 1, pp. 43-43, January 1997.

[17] V. V. Vadlamudi, O. Gjerde and G. Kjolle, "Dependability and security-based failure considerations in protection system reliability studies," IEEE PES ISGT Europe 2013, Lyngby, 2013, pp. 1-5.

[18] H. Ren, I. Dobson, and B.A., Carreras, "Long-Term Effect of the n-1 Criterion on Cascading Line Outages in an Evolving Power Transmission Grid," IEEE Trans. Power Syst., vol.23, no.3, pp.1217,1225, Aug. 2008.

[19] G. Granelli, et al., "Optimal network reconfiguration for congestion management by deterministic and genetic algorithms," Elect. Power Syst. Res., vol.76, no.6-7, pp.549–556, Apr. 2006.

[20] A.R. Escobedo, E. Moreno-Centeno, K.W. Hedman, "Topology Control for Load Shed Recovery," IEEE Trans. Power Syst., vol.29, no.2, pp.908,916, March 2014.

[21] W. Shao and V. Vittal, "Corrective switching algorithm for relieving overloads and voltage violations," IEEE Trans. Power Syst., vol. 20, no. 4, pp. 1877–1885, Nov. 2005.

[22] K. W. Hedman, et al., "Smart flexible just-in-time transmission and flowgate bidding," IEEE Trans. Power Syst., vol. 26, no. 1, pp. 93–102, Feb. 2011.

[23] H. Pandzic, A. J. Conejo, I. Kuzle and E. Caro, "Yearly Maintenance Scheduling of Transmission Lines Within a Market Environment," in IEEE Transactions on Power Systems, vol. 27, no. 1, pp. 407-415, Feb. 2012.

[24] Y. Fu, M. Shahidehpour, and Z. Li, “Security-constrained optimal coordination of generation and transmission maintenance outage scheduling,” IEEE Trans. Power Syst., vol. 22, no. 3, pp. 1302–1313, Aug. 2007.

[25] M. Kezunovic, et al., "Reliable Implementation of Robust Adaptive Topology Control," International Conference on System Sciences (HICSS), 2014 47th Hawaii, vol., no., pp.2493,2502, 6-9 Jan. 2014.

[26] M. Tasdighi and M. Kezunovic, "Impact analysis of network topology change on transmission distance relay settings," 2015 IEEE Power & Energy Society General Meeting, Denver, CO, 2015, pp. 1-5.

[27] M. Tasdighi and M. Kezunovic, "Automated Review of Distance Relay Settings Adequacy After the Network Topology Changes," in IEEE Transactions on Power Delivery, vol. 31, no. 4, pp. 1873-1881, Aug. 2016.

[28] J. A. Peças Lopes, et al., “Integrating distributed generation into electric power systems: A review of drivers, challenges and opportunities,” Elect. Power Syst. Res., vol. 77, no. 9, pp. 1189–1203, Jul. 2007.

[29] R. A. Walling and N. W. Miller, ‘Distributed generation islanding Implications on power system dynamic performance’, in Proc. IEEE/PES Summer Power Meeting, Chicago, IL, July 2002.

[30] M. Tasdighi, M. Kezunovic, ‘Preventing transmission distance relays maloperation under unintended bulk DG tripping using SVM-based approach,’ Electr. Power Syst. Res. 142 (2017) 258–267.

[31] D. M. MacGregor, A. T. Giuliante, and Patterson, "Automatic relay setting," J. of Elec. And Elect. Eng., vol. 21, no. 3, pp. 169-179, 2002.

[32] NERC, "1200 MW Fault Induced Solar Photovoltaic Resource Interruption Disturbance Report," Tech. Rep., June 2017, [Online] Available: http://www.nerc.com.

[33] M. Henderson, Impacts of Transmission System Contingencies on Distributed Generation – Overview, ISO New-England DG forecast group meeting, Dec. 2013. http://www.cancerresearchuk.org/aboutcancer/statistics/cancerstatsreport/

[34] NERC Standard for Generator Frequency and Voltage Protective Relay Settings, NERC Standard PRC-024-2.

[35] S. Eftekharnejad, et al., Impact of increased penetration of photovoltaic generation on power systems, IEEE Transactions on Power Systems, vol. 28, no. 2, pp. 893-901, May 2013.

[36] Adjustment Period and Real-Time Operation, ERCOT Nodal Protocol, http://www.ercot.com/content/wcm/libraries/105131/September_1__2016_Nodal_Protocols.pdf

[37] NERC Standard for Transmission System Planning Performance Requirements, NERC Standard TPL-001-4.

[38] A. Gopalakrishnan, et al., "Simulating the Smart Electric Power Grid of the 21st Century–Bridging the Gap between Protection and Planning," Western Protective Relay Conference, 2013.

[39] M. Kezunovic and C. Zheng, "Monitoring Power System Dynamic Performance Using Synchronized Sampling," CIGRE International Conference on Advances in Power System Control, Operation and Management (APSCOM), St. Petersburg, Russia, April 2008.

[40] M. Kezunovic, B. Matic Cuka, "Hierarchical Coordinated Protection with High Penetration of Smart Grid Renewable Resources (2.3)," PSerc/DOE Workshop, Madison, WI, May 2013.

[41] M. Kezunovic, P. Chen, A. Esmaeilian, and M. Tasdighi," Hierarchically Coordinated Protection: An Integrated Concept of Corrective, Predictive, and Inherently Adaptive Protection," CIGRE International Conference on Actual Trends in Development of Power System Relay Protection and Automation, Sochi, Russia, June 2015.

[42] M. J. Damborg, R. Ramaswami, S.S. Venkata and J.M. Postforoosh, “Computer aided transmission protection system design Part I &II,” IEEE Vol. PAS 103, Jan 1984, pp. 51-59.

[43] R. Ramaswami, “Transmission Protective Relay Coordination- A Computer-Aided-Engineering Approach for Subsystems and Full Systems,” Ph.D Dissertation, University of Washington Seattle, January 1986.

[44] R. E. Albrecht, M. J. Nisja, W. E. Feero, G. D. Rockefeller and C. L. Wagner, "Digital Computer Protective Device Co-ordination Program I-General Program Description," in IEEE Transactions on Power Apparatus and Systems, vol. 83, no. 4, pp. 402-410, April 1964.

[45] S. S. Begian, et al., "A Computer Approach to Setting Overcurrent Relays in a Network," IEEE PICA Conference Record, Vol. 31C69, May 1967, pp. 447-457.

[46] R. B. Gastineau, R. H. Harris, W. L. Woodside and W. V. Scribner, "Using the computer to set transmission line phase distance and ground back-up relays," in IEEE Transactions on Power Apparatus and Systems, vol. 96, no. 2, pp. 478-484, Mar 1977.

[47] A. Ferrero, S. Sangiovannai, E. Zapitelli, 'A Fuzzy set approach to fault type identification in digital relaying', IEEE Trans. Power Delivery 10 (1995) 169–175.

[48] B. Das, J. Vittal Reddy, 'Fuzzy-logic-based fault classification scheme for digital distance protection', IEEE Trans. Power Delivery 20 (2005) 609–616.

[49] P.K. Dash, S.R. Samantray, 'An accurate fault classification algorithm using a minimal radial basis function neural network', Eng. Intelligent Syst. 4 (2004) 205–210.

[50] F. Martin, J.A. Aguado, 'Wavelet based ANN approach for transmission line protection', IEEE Trans. Power Delivery 18 (2003) 1572–1574.

[51] N. Zhang, M. Kezunovic, 'Transmission line boundary protection using wavelet transform and Neural Network', IEEE Trans. Power Delivery 22 (2007) 859–869.

[52] P.K. Dash, A.K. Pradhan, G. Panda, 'Application of minimal radial basis function neural network to distance protection', IEEE Trans. Power Delivery 16 (2001) 68–74.

[53] Y. H. Song, Q. Y. Xuan, and A. T. Johns, 'Protection of scheme for EHV transmission systems with thyristor controlled series compensation using radial basis function neural networks', Elect. Mach. Power Syst., vol. 25, pp. 553—565, 1997.

[54] Y. H. Song, A. T. Johns, and Q. Y. Xuan, Articial 'neural network based protection scheme for controllable series-compensated EHV transmission lines', Proc. Inst. Elect. Eng., Gen. Transm. Distrib., vol. 143, no. 6, pp. 535—540, 1996.

[55] P.K. Dash, S.R. Samantaray, G. Panda, "Fault Classification and Section Identification of an Advanced Series-Compensated Transmission Line Using Support Vector Machine," IEEE Transactions on Power Delivery, vol.22, no.1, pp.67-73, Jan. 2007.

[56] B. Ravikumar, et.al., "Application of support vector machines for fault diagnosis in power transmission system," Generation, Transmission & Distribution, IET, vol.2, no.1, pp.119,130, January 2008.

[57] B. Ravikumar, et.al., "An approach using support vector machines for distance relay coordination in transmission system," IEEE Trans. Power Del., vol. 24, no. 1, pp. 79–88, Jan. 2009.

[58] B. Ravikumar, et.al., "Comparison of Multiclass SVM Classification Methods to Use in a Supportive System for Distance Relay Coordination," IEEE Transactions on Power Delivery, vol.25, no.3, pp.1296-1305, July 2010.

[59] U.B. Parikh, B. Das, and R.P. Maheshwari, "Combined Wavelet-SVM Technique for Fault Zone Detection in a Series Compensated Transmission Line," IEEE Transactions on Power Delivery, vol.23, no.4, pp.1789-1794, Oct. 2008.

[60] A. Ukil, "Intelligent Systems and Signal Processing in Power Engineering," Heidelberg, Berlin, Germany: Springer, pp. 161-226, Dec. 2007.

[61] M. Kezunovic and B. Perunicic, “Fault Location,” in Wiley Encyclopedia of Electrical and Electronics Terminology. New York, USA: Wiley, 1999, vol. 7, pp. 276–285.

[62] IEEE Guide for Determining Fault Location on the Transmission and Distribution Lines, IEEE C37.144-2004.

[63] T. Takagi, Y. Yamakoshi, M. Yamaura, R. Kondow, and T. Matsushima, “Development of a new type fault locator using the one-terminal voltage and current data,” IEEE Trans. Power App. Syst., vol. PAS-101, no. 8, pp. 2892–2898, Aug. 1982.

[64] L. Eriksson, M. Saha, and G. D. Rockefeller, “An accurate fault locator with compensation for apparent reactance in the fault resistance resulting from remote end infeed,” IEEE Trans. Power App. Syst., vol. PAS-104, no. 2, pp. 424–436, Feb. 1985.

[65] A. Johns and S. Jamali, “Accurate fault location technique for power transmission lines,” Proc. Inst. Elect. Eng., Gen., Transm. Distrib., vol. 137, no. 6, pp. 395–402, Nov. 1990.

[66] D. Novosel, D. G. Hart, E. Udren, and J. Garitty, “Unsynchronized two-terminal fault location estimation,” IEEE Trans. Power Del., vol. 11, no. 1, pp. 130–138, Jan. 1996.

[67] A. A. Gigris, D. G. Hart, and W. L. Peterson, “A new fault location technique for two- and three-terminal lines,” IEEE Trans. Power Del., vol. 7, no. 1, pp. 98–107, Jan. 1992.

[68] M. Kezunovic, B. Perunicic, and J. Mrkic, “An accurate fault location algorithm using synchronized sampling,” Elect. Power Syst. Res. J., vol. 29, no. 3, pp. 161–169, May 1994.

[69] A. Gopalakrishnan, M. Kezunovic, S.M.McKenna, and D.M. Hamai, “Fault location using distributed parameter transmission line model,” IEEE Trans. Power Del., vol. 15, no. 4, pp. 1169–1174, Oct. 2000.

[70] P. Dutta, A. Esmaeilian, and M. Kezunovic, "Transmission-Line Fault Analysis Using Synchronized Sampling," in IEEE Transactions on Power Delivery, vol. 29, no. 2, pp. 942-950, April 2014.

[71] Rep. “Determination and Application of Practical Relaying Loadability Rating Version 1,” NERC, June, 2008.

[72] O. Alsac, B. Stott, and W. F. Tinney, "Sparsity-Oriented Compensation Methods for Modified Network Solutions," IEEE Trans. Power App. and Sys., vol.PAS-102, no.5, pp.1050,1060, May 1983.

[73] Power System Test Case Archive, Univ. Washington, Dept. Elect. Eng., 2013. [Online]. Available: https://www.ee.washington.edu/re- search/pstca/index.html.

[74] Alberta Electric System Operator (AESO) [Online]. Available: http://www.aeso.ca/transmission/261.html.

[75] ARPA-E Robust Adaptive Transmission Control (RATC) Project granted under GENI contract 0473-1510, ARPA-E award number DE-AR0000220, [Online]. http://smartgridcenter.tamu.edu/ratc/web/

http://arpa-e.energy.gov/?q=slick-sheet-project/automated-grid-disruption-response-system

[76] High performance research computing (HPC) [Online]. Available: http://sc.tamu.edu.

[77] M. Tasdighi, et.al., "Residential Microgrid Scheduling Based on Smart Meters Data and Temperature Dependent Thermal Load Modeling," IEEE Trans. Smart Grid, vol.5, no.1, pp.349-357, Jan. 2014.

[78] IEEE Standard for Interconnecting Distributed Resources with Electric Power Systems, IEEE Standard 1547-2003, 2003.

[79] IEEE Recommended Practice for Utility Interface of Photovoltaic (PV) Systems, IEEE Standard 929-2000, Jan. 2000.

[80] Standard for Inverters, Converters, and Controllers for Use in Independent Power Systems, UL Standard 1741, Underwriters Laboratories Inc., May 1999.

[81] New York State Standardized Interconnection Requirements, Application Process, Contract and Application Forms for New Distributed Generators, 300 Kilovolt-Amperes or Less, Connected in Parallel with Radial Distribution Lines, New York State Public Service Commission, Nov. 2000.

[82] Rule 21 – Generating Facility Interconnections, California Public Utilities Commission, 2000.

[83] Texas Public Utility Commission Requirements for Pre-Certification of Distributed Generation Equipment by a Nationally Recognized Testing Laboratory, Public Utility Commission of Texas, Feb. 2001.

[84] B. Matic-Cuka, M. Kezunovic, "Islanding Detection for Inverter-Based Distributed Generation Using Support Vector Machine Method," IEEE Transactions on Smart Grid, vol.5, no.6, pp.2676-2686, Nov. 2014.

[85] S.P. Chowdhury, et.al., "Islanding protection of active distribution networks with renewable distributed generators: A comprehensive survey," Electric Power Systems Research, Volume 79, Issue 6, June 2009, Pages 984-992.

[86] V. Vapnik, "The Nature of Statistical Learning Theory (Information Science and Statistics)," New York, NY, USA: Springer, Dec. 1999.

[87] J. Weston and C. Watkins, "Multi-class support vector machines," Dept. Comput. Sci., Royal Holloway, Univ. London, Egham, U.K., Tech. Rep. CSD-TR-98-04, 1998. [Online]. Available: http://citeseer. ist.psu.edu/article/weston98multiclass.html

[88] C-C. Chang and C-J. Lin, LIBSVM: a library for support vector machines. ACM Transactions on Intelligent Systems and Technology, 2:27:1-27:27, 2011. [Online]. Available: http://www.csie.ntu.edu.tw/~cjlin/libsvm

[89] S. S. Keerthi and C.-J. Lin. Asymptotic behaviors of support vector machines with Gaussian kernel. Neural Computation, 15(7):1667-1689, 2003.

[90] H.-T. Lin and C.-J. Lin. A study on sigmoid kernels for SVM and the training of non-PSD kernels by SMO-type methods. Technical report, Department of Computer Science, National Taiwan University, 2003. [Online]. Available: http://www.csie.ntu.edu.tw/~cjlin/papers/tanh.pdf.

[91] J.G. Slootweg, et. al., Modeling new generation and storage technologies in power system dynamics simulations, Proceedings IEEE Summer Meeting, Chicago, July 2002.

[92] M. M. Eissa, et al., A Novel Back Up Wide Area Protection Technique for Power Transmission Grids Using Phasor Measurement Unit, IEEE Transactions on Power Delivery, vol. 25, no. 1, pp. 270-278, Jan. 2010.

[93] IEEE Standard for Synchrophasor Data Transfer for Power Systems, in IEEE Std C37.118.2-2011 (Revision of IEEE Std C37.118-2005).

[94] R. Hasan, et al., Analyzing NASPInet data flows, Power Systems Conference and Exposition, 2009. PSCE '09. IEEE/PES, Seattle, WA, 2009, pp. 1-6.

[95] Power System Test Case Archive, Univ. Washington, Dept. Elect. Eng., 2013. [Online]. Available: https://www.ee.washington.edu/re- search/pstca/index.html

[96] C.-W. Hsu, C.-C. Chang, and C.-J. Lin. A practical guide to support vector classification. [Online]. Available: http://www.csie.ntu.edu.tw/~cjlin/papers/ libsvm.pdf

[97] Roland Nylen, "Auto-reclosing" Repringt from ASEA Journal 1979.6, pp. 127-132.

[98] IEEE Std. C37.104-2012, IEEE Guide for Automatic Reclosing of Circuit Breakers for AC Distribution and Transmission Lines.